

pubs.acs.org/jmc Article

# Structural Determinants of Indole-2-carboxamides: Identification of Lead Acetamides with Pan Antimycobacterial Activity

Pankaj Bhattarai,<sup>#</sup> Pooja Hegde,<sup>#</sup> Wei Li, Pavan Kumar Prathipati, Casey M. Stevens, Lixinhao Yang, Hinman Zhou, Amit Pandya, Katie Cunningham, Jenny Grissom, Mariaelena Roman Sotelo, Melanie Sowards, Lilian Calisto, Christopher J. Destache, Sonia Rocha-Sanchez, James C. Gumbart, Helen I. Zgurskaya, Mary Jackson, and E. Jeffrey North\*



Cite This: J. Med. Chem. 2023, 66, 170-187



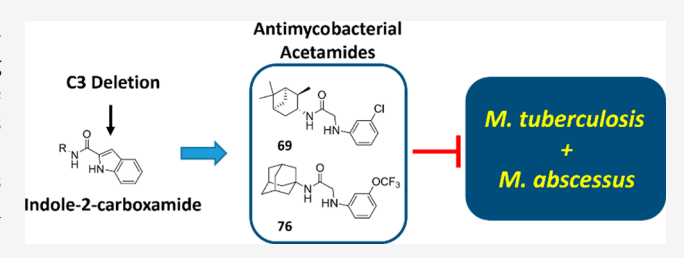
ACCESS

Metrics & More

Article Recommendations

Supporting Information

**ABSTRACT:** Tuberculosis (TB), caused by *Mycobacterium tuberculosis* (*M.tb*), is one of the leading causes of death in developing countries. Non-tuberculous mycobacteria (NTM) infections are rising and prey upon patients with structural lung diseases such as chronic obstructive pulmonary disease (COPD) and cystic fibrosis. All mycobacterial infections require lengthy treatment regimens with undesirable side effects. Therefore, new antimycobacterial compounds with novel mechanisms of action are urgently needed. Published indole-2-carboxamides (IC) with suggested inhibition of



the essential transporter MmpL3 showed good potency against whole-cell *M.tb*, yet had poor aqueous solubility. This project focused on retaining the required MmpL3 inhibitory pharmacophore and increasing the molecular heteroatom percentage by reducing lipophilic atoms. We evaluated pyrrole, mandelic acid, imidazole, and acetamide functional groups coupled to lipophilic head groups, where lead acetamide-based compounds maintained high potency against mycobacterial pathogens, had improved *in vitro* ADME profiles over their indole-2-carboxamide analogs, were non-cytotoxic, and were determined to be MmpL3 inhibitors.

#### ■ INTRODUCTION

Tuberculosis (TB) is a granulomatous infection caused by the bacterial pathogen *Mycobacterium tuberculosis* (*M.tb*). An estimated 10 million people become infected with TB each year worldwide. TB is one of the top 10 causes of death from a single infectious agent, exceeding human immunodeficiency virus—acquired immune deficiency syndrome (HIV-AIDS). The emergence of drug-resistant strains of *M.tb* and the HIV pandemic have made the management of TB more difficult. The treatment success rates have been reported averaging 85% and 56% for drug-susceptible and multi-drug-resistant TB (MDR-TB), respectively. Whereas, for extensively drug-resistant TB (XDR-TB), the treatment success rate was 39%.

On the other hand, prevalence and infection rate with non-tuberculous mycobacteria (NTM) are constantly rising. Although NTM can be non-pathogenic, a few NTM species, including *M. abscessus* complex (MABSC), *M. avium* complex (MAC), and *M. fortuitum*, are opportunistic pathogens that infect patients with structural lung disorders, including chronic obstructive pulmonary disease (COPD), bronchiectasis, and cystic fibrosis.<sup>3,4</sup> According to a published report by Lin et al., the prevalence of NTM infections increased drastically from 0.5% (in 2007) to 11% (in 2011).<sup>5</sup> Additionally, there was a reported increase in MAC- and MABSC-related pulmonary infections by 13% and 24%, respectively, between 1994 and 2014 in Spain.<sup>6</sup> The current NTM therapy is long and

expensive, and includes multi-drug therapy with a combination of intravenous and oral antibiotics that are routinely ineffective, supporting the notion that new NTM agents are strongly needed.

Novel antimycobacterial agents to address these limitations in TB and NTM therapy are critical to effective therapies. The currently available antimycobacterial drugs that act on various targets in mycobacteria are failing due to the development of drug resistance. Hence, several other vulnerable targets in mycobacteria have been identified. Among the potential targets that have been identified in recent times, mycobacteria membrane protein Large 3 (MmpL3) has been shown to be a promising target.

MmpL3 is a mycobacterial membrane protein of the resistance nodulation cell division (RND) family. MmpL3 consists of 944 amino acids and 12 transmembrane domains. The inhibition of MmpL3 prevents the transport of mycolic acid in the form of trehalose monomycolate (TMM) from the

Received: March 4, 2022 Published: December 23, 2022





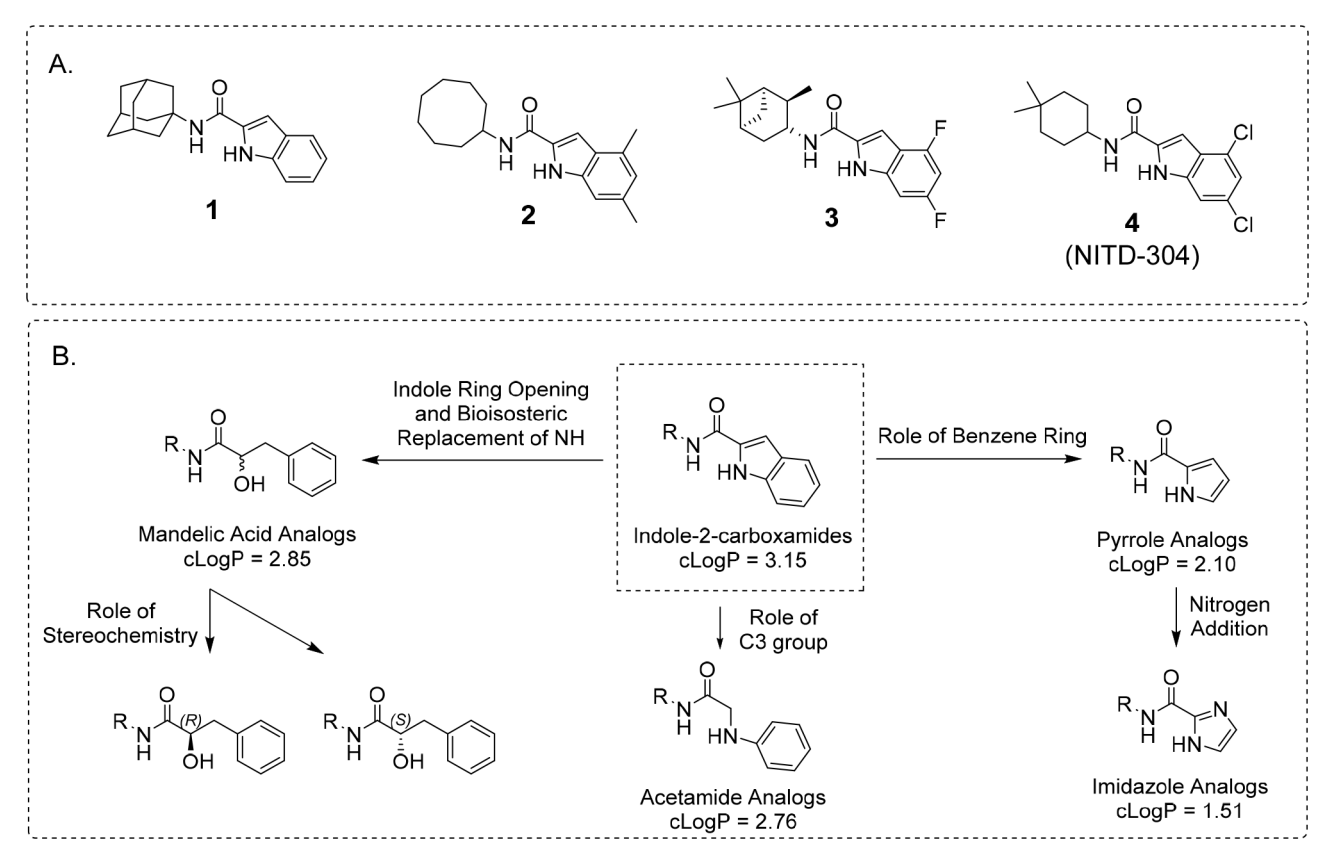


Figure 1. Panel A — Lead IC with highly potent antimycobacterial activity. Panel B — Medicinal chemistry strategy to enhance aqueous solubility. cLogP values are generated where R = cyclooctyl.

inner membrane to the outside of the cell wall, <sup>11</sup> which results in the inhibition of cell growth. A number of chemical scaffolds have been claimed to inhibit this transporter. <sup>12</sup> Inhibition of MmpL3 *in vivo* by indole-based scaffolds has resulted in significant protection against *M.tb-* and *M. abscessus-*infected mouse models, supporting the high translational potential of this target by these scaffolds. <sup>13–17</sup> Thus, MmpL3 is a novel drug target, and an ideal pharmaceutical drug candidate that inhibits this target would potentially address the liabilities in the current anti-TB and anti-NTM therapies.

New chemical entities that retain the essential pharmacophore requirements as MmpL3 inhibitors with enhanced pharmacokinetic profiles should lead to more ideal preclinical drug candidates. In this report, we have evaluated the molecular determinants of the indole-2-carboxamide (IC) class of antimycobacterials in four miniseries (pyrrole-, imidazole-, acetamide-, and mandelic acid-based) using rational drug design and bioisosteric replacement (Figure 1, panel B). The primary design drivers of our new miniseries were to maintain/enhance antimycobacterial potency and improve the lipophilicity/hydrophilicity balance, thereby potentially improving in vivo pharmacokinetic properties, and maintaining a safe pharmacological profile. 18 The current work identified lead acetamide analogs 7,14,16,17,19-21 that maintain the MmpL3 inhibitory pharmacophore while decreasing the percentage of lipophilic carbon atoms, thus retaining potent antimycobacterial activity and significantly increasing aqueous solubility.

#### ■ RESULTS AND DISCUSSION

**Chemistry.** Standard coupling conditions were used to synthesize the pyrrole-, imidazole-, and mandelic acid-based analogs (Scheme 1). Briefly, the substituted carboxylic acids were reacted under  $N_2$  atmosphere with an alkyl- or cycloalkylamine in the presence of 1-ethyl-3-(3-(dimethylamino)propyl)carbodiimide hydrochloride (EDC·HCl), hydroxybenzotriazole (HOBt), and triethylamine (TEA).

Scheme 1. Synthesis of Mandelic Acid, Pyrrole, and Imidazole Analogs<sup>a</sup>

$$R_{\cdot NH_{2}} + HO R_{1} \xrightarrow{a} R_{\cdot N} R_{1}$$

$$R_{1} = N R_{\cdot N} R_{1}$$

$$R_{1} = N R_{\cdot N} R_{1}$$

$$R_{1} = R_{\cdot N} R_{1}$$

$$R_{1} = R_{\cdot N} R_{1}$$

"Reagents and conditions: (a) HOBt, EDC, TEA, cycloaliphatic amine, DMF, r.t., overnight.

Acetamides (Scheme 2) were synthesized by reacting commercially available bulky cycloaliphatic amines with bromoacetyl bromide in the presence of TEA at 0 °C, forming the acetamide intermediate 1a. The *N*-cycloalkyl-2-bromoacetamide intermediates (1a) were then reacted with substituted aniline analogs in the presence of TEA under reflux conditions, yielding acetamide final products (2a). The overall percentage yields were 25%–70%.

Scheme 2. Synthetic Pathway to Produce the Acetamide Series<sup>a</sup>

$$Br \xrightarrow{O} Br + H_2N \xrightarrow{R} Br \xrightarrow{O} R \xrightarrow{D} R_2 \xrightarrow{N} HN-R$$

$$1a \qquad 2a$$

"Reagents and conditions: (a) triethylamine (TEA), dichloromethane (DCM), 0 °C, 4 h; (b) aniline analogs, TEA, THF, 60 °C, overnight.

Antimycobacterial Activity. Each miniseries was evaluated for their antimycobacterial activity against various tuberculous and NTM species, including *M. abscessus*, *M. smegmatis*, and *M.tb*. We synthesized and evaluated seven pyrrole- and imidazole-based compounds and 18 mandelic acid-based compounds with various lipophilic head groups. Generally, these series had modest activity against *M.tb* and *M. abscessus*, where structures, MIC values, cLogP values, and ADME properties along with structure—activity relationship (SAR) discussion can be found in the Supporting Information.

Acetamide Series. Published indole-based compounds have high potency with sub  $\mu g/mL$  minimum inhibitory concentration (MIC) values against mycobacterial pathogens but have poor physicochemical and pharmacokinetic profiles which will likely limit their translational potential (Figure 1, Panel A). Therefore, we attempted to optimize indole-based scaffolds to enhance the aqueous solubility, retain high antimycobacterial activity and improve pharmacokinetic profiles by reducing lipophilic atoms in the scaffold. In addition, our approach was to "open" the indole ring by removal of the lipophilic 3-CH group as shown in Figure 1, yielding the acetamide series to enhance aqueous solubility while retaining the pharmacophoric requirement of indole-based compounds. Recently, Shetty et al. have identified an acetamide targeting MmpL3 through a high-throughput screen.<sup>22</sup> However, further extensive optimization of acetamides is necessary to find a successful clinical drug candidate.

The acetamides compared to the parent indole-based compounds have (a) effectively increased the heteroatom percentage, (b) reduced lipophilicity by removal of the lipophilic 3-CH group, and (c) increased 3D sp³ characteristics, thereby reducing planarity and decreasing the crystal lattice energy of the planar structure, leading to enhanced aqueous solubility as solvation energy gets increased relatively. <sup>23–25</sup>

**SAR of Acetamide Scaffold.** The cyclooctyl, cycloheptyl, and transmethylcyclohexyl head groups (37, 38, and 39, respectively) were inactive, with MIC values of  $\geq$ 64  $\mu$ g/mL against both the *M. abscessus* and *M.tb* strains. The acetamide with the (1R,2R,3R,5S)-(—)-isopinocampheyl head group (40) exhibited the highest activity among all the unsubstituted anilines, with an MIC value of 8  $\mu$ g/mL against both *M. abscessus* and *M.tb*. The 1-adamantyl head-group-substituted acetamide (41) also exhibited some activity against *M. abscessus* (16  $\mu$ g/mL) and *M.tb* (32  $\mu$ g/mL). However, the 2-adamantyl head group (42) was inactive against *M. abscessus* but moderately active against *M.tb* (16  $\mu$ g/mL).

The chloro, bromo, methyl, methoxy, trifluoromethyl, and trifluoromethoxy functional groups were substituted at the *para*-position on aniline to initially and further evaluate the SAR of acetamides. The most active acetamide among unsubstituted anilines, (1R,2R,3R,5S)-(-)-isopinocamphane (40), was chosen for substitution of functional groups at the

para-position on aniline. The para-position was chosen to be evaluated since CYP-mediated para-hydroxylation is a common metabolic reaction on phenyl rings. Compounds para-substituted with chloro or bromo groups had 2-fold enhanced activity against M. abscessus over the unsubstituted analog (40), but no improvement against M.tb. The paramethyl substitution (45) did not show any increased potency as compared to its unsubstituted counterpart; however, the para-methoxy substituted analog decreased activity against both the strains. The para-trifluoromethyl substitution, 48, did not exhibit significant activity, whereas para-trifluoromethoxyaniline, 47, achieved the highest activity in this series against M. abscessus and M.tb, with MIC values of  $1 \mu g/mL$  and  $4 \mu g/mL$ , respectively.

The six para-substituted aniline analogs were also evaluated with the 1-adamantyl head group. The para-chloro-substituted compound (49) was 2- and 4-fold more potent than unsubstituted counterpart against M.tb and M. abscessus, respectively. Similarly, the bromo-substituted compound (50), was more potent than para-chloro substitutions by 2fold for both M. abscessus and M.tb. This suggested that bulky, electron-withdrawing, and lipophilic para-substitutions also resulted in increased activity, even more so with the 1adamantyl head group. The para-methyl and para-methoxy analogs (51 and 52) resulted in decreased activity. The trifluoromethoxy substitution with 1-adamantyl head group (53) resulted in an augmented activity with 8-fold increment against M. abscessus and 2-fold increment against M.tb. The trifluoromethyl substitution with 1-adamantyl head group (54) also resulted in an increased activity compared to unsubstituted aniline. Similar to the (1R,2R,3R,5S)-(-)-isopinocamphane series, bulky, electron-withdrawing, and lipophilic groups at the para-position were optimal for antimycobacterial activity.

The six para-substituted anilines were also evaluated with the 2-adamantyl head group, that achieved moderate to low antimycobacterial activity in the unsubstituted series. A similar SAR was seen in 2-adamantyl-substituted compounds compared to (1R,2R,3R,5S)-(-)-isopinocampheyl- and 1adamantyl-substituted compounds. Despite the para-chlorosubstituted aniline (55) being inactive, the para-bromosubstituted aniline (56) was 16-fold more potent against M. abscessus and 4-fold more potent against M.tb in comparison to unsubstituted aniline (42). The trifluoromethyl-substituted aniline (60, M. abscessus MIC = 4  $\mu$ g/mL, M.tb MIC = 2  $\mu$ g/ mL) and trifluoromethoxy-substituted aniline (59, M. abscessus MIC = 2  $\mu$ g/mL, M.tb MIC = 4  $\mu$ g/mL) exhibited good potencies against both the strains. Aside from the para-chloro analog being inactive, which is contrary to the established SAR from the (1R,2R,3R,5S)-(-)-isopinocampheyl and 1-adamantyl series, bulky, electron-withdrawing, and lipophilic substituents were optimal for antimycobacterial activity.

In an effort to determine if *para*-substituted aniline groups could restore the antimycobacterial activity of the cyclooctyl head group, which is arguably the most potent head group across a panel of mycobacterial pathogens in the indole series, six compounds with this head group were tested for their antimycobacterial activity. The cyclooctyl head group did not exhibit significant activity regardless of the identity of any substitutions on the aniline moiety. As expected, the bulky, electron-withdrawing, and lipophilic chloro substituent (61) achieved modest activity against *M. abscessus* (32  $\mu$ g/mL) but not against *M.tb*. In addition, the trifluoromethoxy substitution

Table 1. Antimycobacterial Activity of Acetamide Scaffold

		37 70	2410/	
Compound	R Bulky Lipophilic Head Group	R <sub>1</sub> Phenyl Ring	MIC (µ M. abscessus ATCC 19977	<i>M.tb</i> H37Rv mc <sup>2</sup> 6206
37			>64	64
38			>64	64
39		3	>64	64
40			8	8
41	Dx		16	32
42	To get		>64	16
43		S. CI	4	16
44		Br	4	16
45	\	\$	8	16
46		F OCH₃	32	64
47		OCF3	1	4
48		CF <sub>3</sub>	32	16
49		₹()-cı	4	16
50		Br	2	8
51	<i></i>	*	32	32
52	1	OCH <sub>3</sub>	32	32
53		OCF <sub>3</sub>	2	16
54		CF <sub>3</sub>	8	8
55		₹\\ CI	>64	64
56		Br	4	4
57	D <sub>x</sub>	*	16	4
58		€ OCH3	32	32
59		OCF <sub>3</sub>	2	4
60		CF <sub>3</sub>	4	2

Table 1. continued

	R		MIC (μg/mL)		
Compound	Bulky Lipophilic Head Group	R <sub>1</sub> Phenyl Ring	M. abscessus ATCC 19977	<i>M.tb</i> H37Rv mc²6206	
61		₹\}_CI	32	64	
62		\$	>64	32	
63	O <sub>z</sub> t	₹ OCH3	>64	64	
64		OCF <sub>3</sub>	8	32	
65		*()	64	32	
66	$\longrightarrow$	₹\cı	>64	64	
67	\\\\\\\\\\\\\\\\\\\\\\\\\\\\\\\\\\\\\\	£ ()	>64	64	
68		CI	1	0.25	
69		CI	0.5	0.25	
70		Br	1	0.5	
71		CI	16	8	
72		CI	1	1	
73		Br	8	8	
74		Br	1	1	
75		F <sub>3</sub> CO	>64	32	
76		OCF <sub>3</sub>	0.5	0.25	
2	N HV		0.063	0.0195	

(64) showed the highest activity against M. abscessus (8  $\mu$ g/mL) and M.tb (32  $\mu$ g/mL). Despite the modest activity seen with the para-chloro and para-trifluoromethoxy groups, no para-substituted aniline was able to appreciably improve the activity with a cyclooctyl head group. The para-substituted anilines were also unable to restore activity with a transmethylcyclohexyl head group. Compounds 67 and 66 possessed trans-methylcyclohexyl head groups with paramethyl substitution and para-chloro substitution, respectively, and both were inactive. This pointed toward the importance of lipophilic and rigid bulky groups in imparting antimycobacterial activity.

After the optimal identity of para-substitutions on the aniline ring was determined, the roles of ortho- and meta-substitutions were determined. The ortho and meta analogs using chloro, bromo, and trifluoromethoxy groups, which exhibited good potencies in either M. abscessus or M.tb (43, 44, 49, 50, and 53), were also screened for their antimycobacterial

activity, as shown in Table 1. These were determined using the two most active head groups (1R,2R,3R,5S)-(-)-isopinocamphane and 1-adamantane. Compounds 68 (M. abscessus MIC = 1  $\mu$ g/mL, *M.tb* MIC = 0.25  $\mu$ g/mL) and **69** (*M*. abscessus MIC = 0.5  $\mu$ g/mL, M.tb MIC = 0.25  $\mu$ g/mL) were ortho-chloro- and meta-chloro-substituted aniline analogs, respectively, with (1R,2R,3R,5S)-(-)-isopinocampheyl head groups and achieved optimal antimycobacterial activity. The increase in activity at the meta-substitutions (bromo and trifluoromethoxy) was seen for all the compounds tested. However, except for compound 68, all other orthosubstitutions (71, 73, and 75) resulted in either a decrease in activity or no change. Compound 70, a meta-bromosubstituted analog with a (1R,2R,3R,5S)-(-)-isopinocamphane head group, was found to have an M. abscessus MIC = 1  $\mu$ g/mL and M.tb MIC = 0.5  $\mu$ g/mL and greater activity than the parasubstituted counterpart (44) by 4-fold against M. abscessus and 32-fold against M.tb. Compound 72 (M. abscessus MIC = 1  $\mu$ g/

Table 2. MIC Values of Lead Acetamides against a Panel of NTM Pathogens

	M. fortuitum	M. avium	M. intracellulare	M. chelonae	M. chimaera	M. kansasii
Compd.	ATCC 6841	subsp. Avium 2285R	1956	ATCC 35752	1501948	ATCC 1279
68	2	16	16	4	>64	16
69	2	8	8	4	16	8
70	2	16	8	8	16	8
76	2	8	8	4	16	8

Table 3. In Vitro ADME-Tox Evaluation

	in vitro ADME values					Cytotoxicity		
				Metabolic Stability $^d(t_{1/2}, h)$			Selectivity Index <sup>f</sup>	
Compd.	Solubility $^a(\mu g/mL)$	Permeability <sup>b</sup> ( $\times 10^{-6}$ cm/s)	HPPB <sup>c</sup> (% bound)	human	mouse	$IC_{50}^{e}(\mu g/mL)$	M.abs	M.tb
50	$1.3 \pm 0.01$	$0.28 \pm 0.04$	99.6 ± 0.14	$2.5 \pm 0.9$	$4.0 \pm 0.1$	>20	>10	>2.5
53	$6.79 \pm 0.5$	$0.47 \pm 0.05$	$99.8 \pm 0.01$	$3.1 \pm 0.1$	$4.1 \pm 0.0$	>20	>10	>1.2
60	$23.9 \pm 0.9$	$0.34 \pm 0.19$	$94.3 \pm 0.5$	$5.8 \pm 0.3$	$15.6 \pm 2.8$	>20	>5	>10
59	$20.3 \pm 0.4$	$3.12 \pm 0.03$	$96.7 \pm 0.01$	$5.9 \pm 0.8$	$3.7 \pm 0.5$	>20	>10	>5
47	$4.5 \pm 0.2$	$3.19 \pm 0.03$	$95.2 \pm 0.05$	$9.2 \pm 6.4$	$4.1 \pm 0.9$	>20	>20	>5
68	$14.3 \pm 0.4$	$0.38 \pm 0.03$	$95.5 \pm 0.1$	$5.1 \pm 0.3$	$8.6 \pm 0.5$	>20	>20	>80
69	$16.3 \pm 0.3$	$1.33 \pm 0.01$	$94.1 \pm 0.02$	$5.3 \pm 0.2$	$4.6 \pm 0.6$	>20	>40	>80
70	$18.6 \pm 0.3$	$1.01 \pm 0.01$	$95.5 \pm 0.1$	$4.2 \pm 3.7$	$5.8 \pm 0.5$	>20	>20	>40
72	$30.3 \pm 1.0$	$0.32 \pm 0.005$	$99.8 \pm 0.01$	$5.6 \pm 3.0$	$1.7 \pm 0.9$	>20	>20	>20
74	$22.2 \pm 1.5$	$1.02 \pm 0.02$	$93.2 \pm 0.1$	$0.5 \pm 0.0$	$ND^g$	>20	>20	>20
76	$20.4 \pm 2.4$	$3.61 \pm 0.04$	$94.9 \pm 0.3$	$0.7 \pm 0.0$	$0.4 \pm 0.1$	>20	>40	>80
2	$1.6 \pm 0.0$	$0.18 \pm 0.09$	$98.2 \pm 0.3$	$0.5 \pm 0.1$	ND	>14.9	>237	>764
Ranitidine	$77.5 \pm 1.8$	$3.47 \pm 0.50$	$20.7 \pm 2.9$	ND	ND	ND	ND	ND

<sup>&</sup>quot;Kinetic solubility assay. "PAMPA permeability assay. "Human plasma protein binding. "Metabolic stability against S9 fraction. "IC<sub>50</sub> values for acetamides were determined against the WI-26 VA4 cell line, and the THP-1 cell line was used for 2. "Selectivity index =  $IC_{50}$ /MIC. "ND = not determined."

mL, M.tb MIC = 1  $\mu$ g/mL) and compound 74 (M. abscessus MIC = 1  $\mu$ g/mL, M.tb MIC = 1  $\mu$ g/mL) were meta-chloro and meta-bromo analogs with 1-adamantyl head groups. Compound 72 exhibited a 4-fold increase in potency against M. abscessus and a 16-fold increase in potency against M.tb compared to its para-substituted counterpart (49). Similarly, compound 76 exhibited a 4-fold increase in potency against M. abscessus and a 64-fold increase in potency against M. abscessus and a 64-fold increase in potency against M. the compared to its para-substituted counterpart, compound 53. These data suggested that the bulky, electron-withdrawing, and lipophilic groups at the meta-position are optimal for antimycobacterial activity.

These results support that bioisosteric replacement from indoles to lead acetamides maintained the required pharmacophore and achieved optimal antimycobacterial potency. The microbiological assessment of the acetamides identified 11 compounds from the acetamides series that have achieved an MIC value of at least 2  $\mu$ g/mL against either M. abscessus or M.tb, with three compounds reaching an MIC value of 0.25  $\mu$ g/mL against M.tb. SAR studies suggest that the 1-adamantane, 2-adamantane, and (1R,2R,3R,5S)-(-)-isopinocamphane head groups were optimal. Bulky, electron-withdrawing, and lipophilic groups in either the meta- or paraposition promoted antimycobacterial activity with meta-substitution being optimal. Generally, ortho-substitutions were detrimental for activity.

To determine spectrum of mycobacterial activity, we further evaluated the antimycobacterial efficacy against a panel of six NTM pathogens (Table 2) of four lead acetamides (68, 69, 70, 76) that achieved an MIC value <1  $\mu$ g/mL against M. abscessus or M.tb. The NTM pathogens evaluated were M. fortuitum, M. avium, M. intracellulare, M. chelonae, M. chimaera, and M.

kansasii. In Table 2, all compounds had similar activity profiles against each NTM pathogen except for 68, which showed no growth inhibition against M. chimaera up to 64  $\mu$ g/mL. All four compounds had the best potency against M. fortuitum and worst against M. chimaera. Overall, lead acetamides were much more active against M. abscessus and M.tb.

*In Vitro* ADME-Tox Studies. *In vitro* evaluations of compounds with MIC  $\leq 2 \mu g/mL$  against *M. abscessus* or *M.tb* were performed (see Table 2).

Aqueous Solubility. There was a 30-fold increase in the aqueous solubility of the acetamides from indoles. The solubility ranged from approximately 2  $\mu$ g/mL to 30  $\mu$ g/mL. Compounds 50, 53, and 47 were the least aqueous soluble compounds, with aqueous solubility value of less than 10  $\mu$ g/ mL. Compounds 68, 69, and 70 exhibited solubility at a range of  $10-20 \mu g/mL$ . The other active compounds, **60**, **59**, **72**, **74**, and 76, demonstrated the highest aqueous solubilities, in the range of 20-30  $\mu$ g/mL (Table 3). The aqueous solubility of the previous generation indoles was typically less than 1  $\mu$ g/ mL, which falls in a category of practically insoluble as defined by the United States Pharmacopeia (USP). There is a definite boost in aqueous solubility profiles by around 30-fold in the acetamide class; however, acetamides also fall in the practically insoluble or insoluble category. Ranitidine was used as a positive control with a reported kinetic aqueous solubility of 79.5  $\mu$ g/mL, <sup>26</sup> and the value obtained experimentally is 77.5  $\pm$  1.8  $\mu$ g/mL, supporting that the described experiment is accurate and reproducible.

PAMPA Permeability. Permeability  $(P_{\rm e})$  above  $0.5 \times 10^{-6}$  cm/s is considered optimal for early stage drug development.<sup>27</sup> Generally, most of the acetamides were found to be moderately permeable, with a small number of compounds

Journal of Medicinal Chemistry

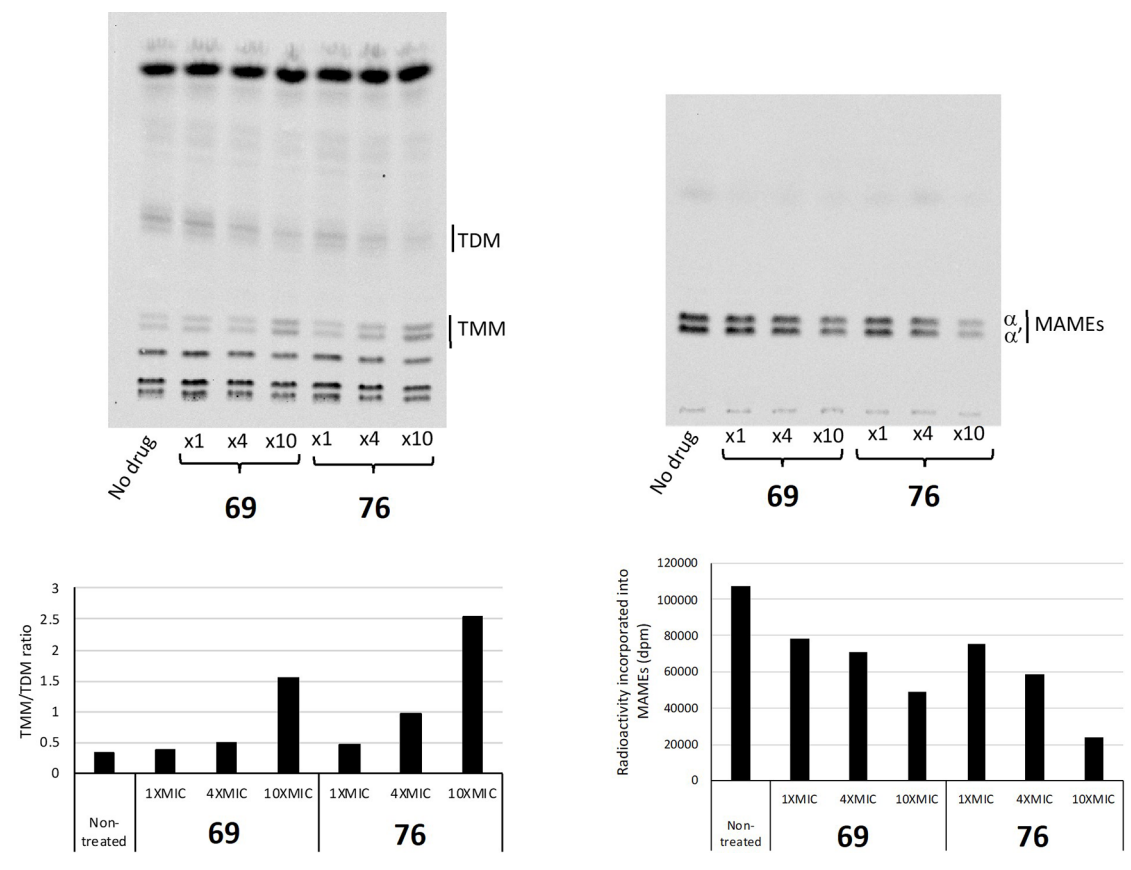


Figure 2. Effect of 69 and 76 on the transfer of mycolic acids onto their cell envelope acceptors in M. abscessus ATCC 19977. Lipid and cell-wall-bound mycolic acid methyl ester (MAME) analysis was performed on untreated and 69- and 76-treated M. abscessus ATCC 19977 cells. Bacterial cultures were treated for 3 h with 1×, 4×, and 10× MIC concentrations of compounds and labeled concomitantly with  $[1,2^{-14}C]$  accetate  $(0.5 \,\mu\text{Ci}/\text{mL};\text{ specific activity 54.3 Ci/mol; Perkin Elmer, Inc.})$ . 20,000 cpm of  $[^{14}C]$  accetate-labeled lipids from each sample was analyzed by TLC in the solvent system  $[CHCl_3:CH_3OH:H_2O, 20:4:0.5]$  and revealed by PhosphorImaging. MAMEs prepared from the same untreated and inhibitor-treated cells (same volume loaded per sample) were analyzed by TLC in the solvent system [n-hexane:ethyl accetate, 95:5; three developments]. The amount of radioactivity incorporated in the products of interest was semi-quantified using a PhosphorImager, and the results are presented as histograms.

found to have low permeability using the parallel artificial membrane permeability assay (PAMPA). Compound 76 showed the highest permeability of  $3.61 \times 10^{-6}$  cm/s, whereas compound **50** showed the lowest permeability of  $0.28 \times 10^{-6}$ cm/s. Compounds 50, 53, 60, 68, and 72 had poor permeability, while compounds 59, 47, 69, 70, 74, and 76 had moderate permeability. Six of the 11 active compounds surpassed this threshold, indicating that acetamides could be further developed from a permeability stance. A new chemical entity (NCE) with a PAMPA permeability profile higher than  $3 \times 10^{-6}$  cm/s would typically be classified as highly permeable according to the Biopharmaceutical Classification System (BCS). Only one compound, 76, has a PAMPA permeability of  $3.5 \times 10^{-6}$ . The other two compounds are between the range of  $2 \times 10^{-6} - 3.5 \times 10^{-6}$  cm/s, which may be developed further to enhance permeability. Ranitidine was used as a positive control for the PAMPA experiments. The reported PAMPA permeability for ranitidine was  $1.4 \times 10^{-6}$ cm/s,<sup>30</sup> and the experimentally determined permeability for ranitidine was  $3.47 \times 10^{-6}$  cm/s.

Human Plasma Protein Binding (HPPB). Results from the rapid equilibrium dialysis (RED) plasma protein binding assays indicate that all the active compounds of the acetamides series were highly protein bound (Table 3). Compounds containing varying substitutions on the aromatic ring of the acetamides

were found to be highly protein bound (>90%). Hence, protein binding patterns may be independent of the variation on the aromatic ring. Acetamides **72**, **53**, and **50** were found to have % bound values of 99.8%, 99.8%, and 99.6%, respectively. Except for these three, all the other compounds fall within the percentage bound range of 93.2% to 96.7%. In summary, the acetamides in the series had high plasma protein binding profiles (94% to 99%). Ranitidine was selected as a positive control for determination of HPPB. Literature values report a value of 15% protein-bound for ranitidine, <sup>26</sup> correlating closely to the experimentally determined value of 20.7%.

Metabolic Stability. Lead acetamides were evaluated for metabolic stability by incubating each compound in human and mouse S9 fraction (Table 3). Ideal metabolic stability is routinely accepted as >30% of compound remaining after 90 min. All compounds tested, except for 74 and 76, had half-lives greater than 2 and 1.7 h in human and mouse S9 fractions, respectively.

*Cytotoxicity.* As an initial evaluation of safety, lead acetamides were tested for cytotoxicity against the human embryonic cell line WI-26 VA4 using the MTT cell viability assay (Table 3). All compounds showed no cytotoxicity up to 20  $\mu$ g/mL. All compounds were able to achieve an excellent selectivity index for *M. abscesses*, except for **60**. Compounds **60**, **68**, **69**, **70**, **72**, **74**, and **76** were able to achieve an excellent

selectivity index for M.tb. In addition, we determined cytoxicity against the HEI-OC1 cell line, which can serve as a surrogate cell line for ototoxicity. We tested **69** and **76** up to 100  $\mu$ M. Acetamide **69** had an IC<sub>50</sub> of 14.13  $\mu$ M, and **76** was significantly less toxic, with 70.8% of cells still viable at the highest concentration.

#### MECHANISM OF ACTION

In particular, acetamide compounds have been reported to target MmpL3 in M.tb, resulting in an inhibition of the transfer of mycolic acids to their major cell envelope acceptors, arabinogalactan and trehalose dimycolates (TDMs).<sup>22</sup> To determine whether the acetamide inhibitors identified herein displayed a similar activity on NTM strains, cultures of M. abscessus ATCC 19977 treated with 1x, 4x, and 10x MIC concentrations of compounds 69 and 76 were metabolically labeled with [1,2-14C] acetate and their lipid and cell-wallbound mycolic acid contents analyzed by thin-layer chromatography (TLC). The MmpL3 transporter is known to shuttle mycolic acids in the form of TMM across the cell membrane. Therefore, MmpL3 inhibitors should elicit an accumulation of TMM intracellularly. Acetamide-based inhibitor treatments did not inhibit mycolic acid biosynthesis per se but resulted in a concentration-dependent build-up of TMM in the cells that accompanied a decrease in mycolic acid transfer onto cell wall arabinogalactan and TDM, thereby pointing to MmpL3 as their target (Figure 2).

Further supporting MmpL3 as the likely bactericidal target of acetamides in *M.tb*, the screening of **69** and **76** against our collection of *M. smegmatismmpL3* knock-out mutants complemented with >80 different mutated or truncated variants of the *mmpL3* gene from *M.tb* (*mmpL3tb*) yielded six strains whose resistance to both compounds was increased 4-fold or more relative to the control strain expressing a wild-type (WT) version of *mmpL3tb* (Table 4). That resistance in these mutants did not result from the overexpression of the mutated

Table 4. MIC (in  $\mu$ g/mL) of 69 and 76 against M.abs ATCC 19977 Isogenic Mutants Expressing Point-Mutated Forms of mmpL3 (M. abscessus Gene)<sup>a</sup>

Mutated MmpL3tb variant expressed in Msmg	69	76	CLA	CIP
MmpL3tb WT	1	0.5	0.5	1
MmpL3tb S309C	8	4	0.5	1
MmpL3tb L189R	4	2	0.5	1
MmpL3tb G253E	4	4	0.5	1
MmpL3tb S288T	16	8	0.5	1
MmpL3tb L567P	2	2	0.5	1
MmpL3tb S591I	4	4	0.5	1
MmpL3tb F644C	4	2	0.5	1
MmpL3tb V684G	2	0.5	0.5	1
MmpL3tb V684A	2	1		
Mabs WT	0.5	0.5	8	1
Mabs MmpL3abs <sup>I306S</sup>	1	1	4	1
Mabs MmpL3abs <sup>A309P</sup>	>64	>64	4	1
Mabs MmpL3abs <sup>L551S</sup>	0.5	0.5	8	1

<sup>&</sup>quot;M. smegmatis mmpL3 knock-out mutant expressing mutated variants of the mmpL3 gene from M.tb. Mutants showing a 4-fold (or greater) increase in MIC to both compounds over their parent control strain (M. smegmatis expressing WT mmpL3tb or M. abscessus ATCC 19977 WT) are in red font. These mutants in red support the importance of the WT residues for inhibitor binding. CLA, clarithromycin; CIP, ciprofloxacin (negative control drugs).

forms of *mmpL3tb* relative to the WT version of the gene was verified by qRT-PCR.<sup>22</sup> The >128-fold increase in MIC of **69** and **76** against an isogenic *M. abscessus* ATCC 19977 mutant harboring a mis-sense mutation in its MmpL3 protein (A309P) (Table 4) is further evidence that this transporter most likely serves as the primary bactericidal target of these compounds in *M. abscessus*.

Two independent approaches were finally used to determine whether 69 or 76 physically interacted with *M.tb* MmpL3. First was a flow-cytometry-based competition binding assay recently developed by our laboratories wherein 69 and 76 were tested for their ability to displace the fluorescent inhibitor probe North 114 (an IC linked with the TAMRA fluorescent fluorophore) in intact *M. smegmatis* bacilli expressing the WT *mmpL3* genes from *M.tb* as its sole copy of this gene. The fluorescence profile of North 114 changes when displaced from MmpL3 by other MmpL3 inhibitors. The results, which are presented in Figure 3, clearly indicate that both 69 and 76 displaced the fluorescent probe, indicating MmpL3 binding.

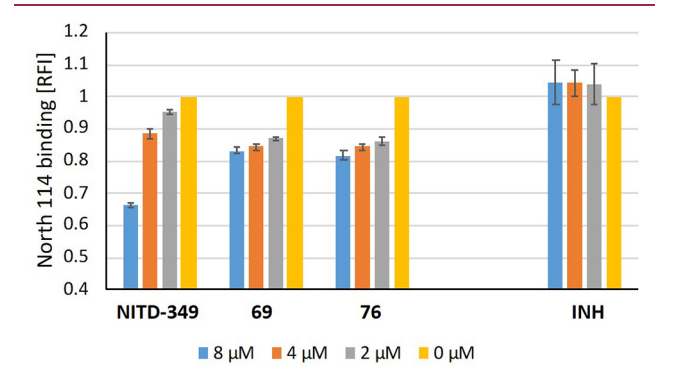
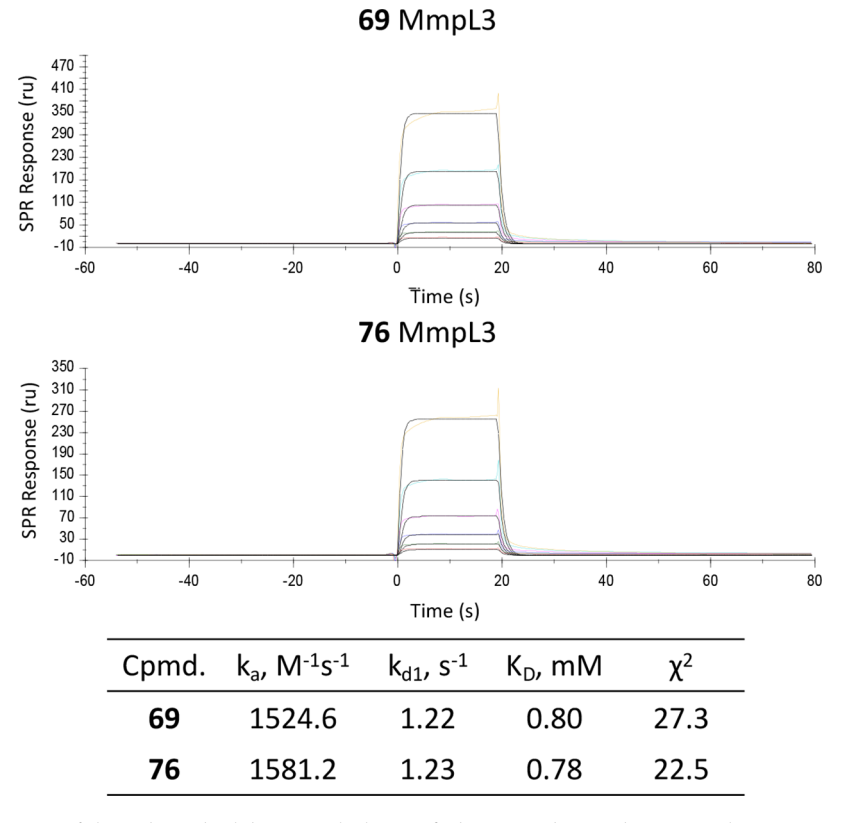


Figure 3. Flow-cytometry-based competition binding assay using intact M. smegmatis cells expressing MmpL3tb. The flow-cytometry-based competition binding assay was performed in an M. smegmatismmpL3 deletion mutant expressing the WT mmpL3tb gene (M. smegmatis-mmpL3/pMVGH1-mmpL3tb). Cells were labeled with 4  $\mu$ M North 114, co-treated with increasing concentrations of 69 and 76, and incubated for 15 min. The concentrations of inhibitors are indicated under the X-axis. Shown on the Y-axis are the mean fluorescence intensities (MFIs) of the bacilli from each treatment group expressed relative to that of bacilli not treated with any inhibitor (relative fluorescence intensity [RFI] value arbitrarily set to 1). MFIs were determined by analyzing 10,000 bacilli under each condition. The data reported are mean values  $\pm$  SD of technical duplicates. NITD-349 is a positive control for probe displacement, while isoniazid (INH) is a negative control.

The direct binding of **69** and **76** to purified MmpL3tb was further confirmed by surface plasmon resonance (SPR) as described in our previous studies with similar binding capabilities to the IC class of MmpL3 inhibitors. <sup>31,32</sup> Briefly, MmpL3 was immobilized on a chip and various concentrations of **69** and **76** were flowed across the immobilized MmpL3 protein. If drug binding to MmpL3 occurs, the conformation change in the protein is detected through refractive index. Compounds **69** and **76** were injected over the purified and immobilized MmpL3tb at 2-fold increasing concentrations from 12.5  $\mu$ M to 400  $\mu$ M. Both **69** and **76** bind to MmpL3tb with fast on and off rates and similar binding affinities in the micromolar range (Figure 4).

Journal of Medicinal Chemistry



**Figure 4.** Kinetics of interactions of the indicated inhibitors with the purified MmpL3tb. Conditions are the same as in Figure 3. Compounds **69** and **76** were injected at 2-fold increasing concentrations from 12.5  $\mu$ M to 400  $\mu$ M at a 20  $\mu$ L/min flow rate in the running buffer containing 25 mM HEPES-KOH (pH 7.4), 150 mM NaCl, 0.2% Triton X-100, 5% DMSO. Sensorgrams (colored lines) are fit globally (black lines) into a 1:1 binding model.

#### ■ MOLECULAR MODELING

In order to rationalize the MmpL3 binding capabilities among lead acetamides, we performed docking studies of **69** and **76** to determine key binding interactions (Figure 5). The docking protocol used was validated by redocking crystallized inhibitors SQ109, ICA38, and NITD-349 to MmpL3 from each of their respective crystal structures. <sup>12,33</sup> The top pose identified for each is very similar to the crystallized one (data not shown).

Acetamides were docked into the published MmpL3 crystal structure (PDB ID: 6AJG) in a similar binding pattern to known MmpL3 inhibitor SQ109. 12,33 SQ109 is a known MmpL3 inhibitor with clinical utility as an orphan drug used in M.tb treatment. Docking results for 76 indicated the hydrophobic interaction between aromatic ring 76 and Ile253, Ile297, Leu642, Leu686 (layer 1); Tyr257, Ala682, Tyr646, Asp645 (layer 2); and Phe260, Phe649 (layer 3); and two H-bonds with Asp645. The interaction between ligand 76 and MmpL3 can be clearly divided into three layers. The hydrophobic interactions in layer 1 are similar to the hydrophobic interactions between SQ109 and layer 2. We note that, in comparing the lengths of SQ109 and 76, 76 is shorter than SQ109, which might be the reason why there is not another layer providing hydrophobic interactions to it as layer 1 for SQ109.

Docking results for 69 showed similar results with a few differences. Layer 1 hydrophobic interactions for the 69 aromatic ring are the same as for the 76 aromatic ring. Layer 2 interactions for 69 include hydrophobic interactions with Tyr646 and Ala682 and only one H-bond with D645. Layer 3 hydrophobic interactions with 69's lipophilic isocampheyl head

group are the same as those with 76's 1-adamantyl head group. An inactive mandelic acid analog substituted with an isocampheyl head group (20 in Supporting Information) was also docked into MmpL3 and was shown to bind to the same site as 69 and 76; however, there were fewer hydrophobic interactions made between inhibitor and MmpL3 in layer 1, which may be the reason for the reduced antimicrobial activity (data not shown).

Compounds 69 and 76 were also docked to MmpL3 structures co-crystallized with ICA38 (PDB ID: 6AJJ) and with NITD-349 (PDB ID: 7C2M), forming nearly conserved interactions compared to the two crystallized compounds. 12,33 ICA38 has a spirocyclohexyl lipophilic head group, and NITD-349 has a 4,4-dimethylcyclohexyl lipophilic head group. These lipophilic head groups make hydrophobic interactions with F260 and F649, as seen with the docked complexes with 69's and 76's lipophilic head groups, which are isocampheyl and 1adamantyl, respectively. All ICs that are MmpL3 inhibitors make a key ion-dipole interaction with D645. This is commonly observed with the amide NH (ICA38 and NITD-349) or with the indole NH (NITD-349). Similarly, the anilino NH's on 69 and 76 make the ion-dipole bond with D645. Additionally, the amide-NH on 76 was also observed to make the ion-dipole bond with D645. Both ICA38 and NITD-349 have the same substituted indole, which is a 4,6-difluoroindole ring. These aromatic rings were shown to primarily make hydrophobic interactions with various isoleucine, leucine, and valine residues. Our lead acetamides lack an indole ring, due to the deletion of the C3 carbon on an indole ring; however, the aromatic anilino ring makes hydrophobic interactions with

**Journal of Medicinal Chemistry** 

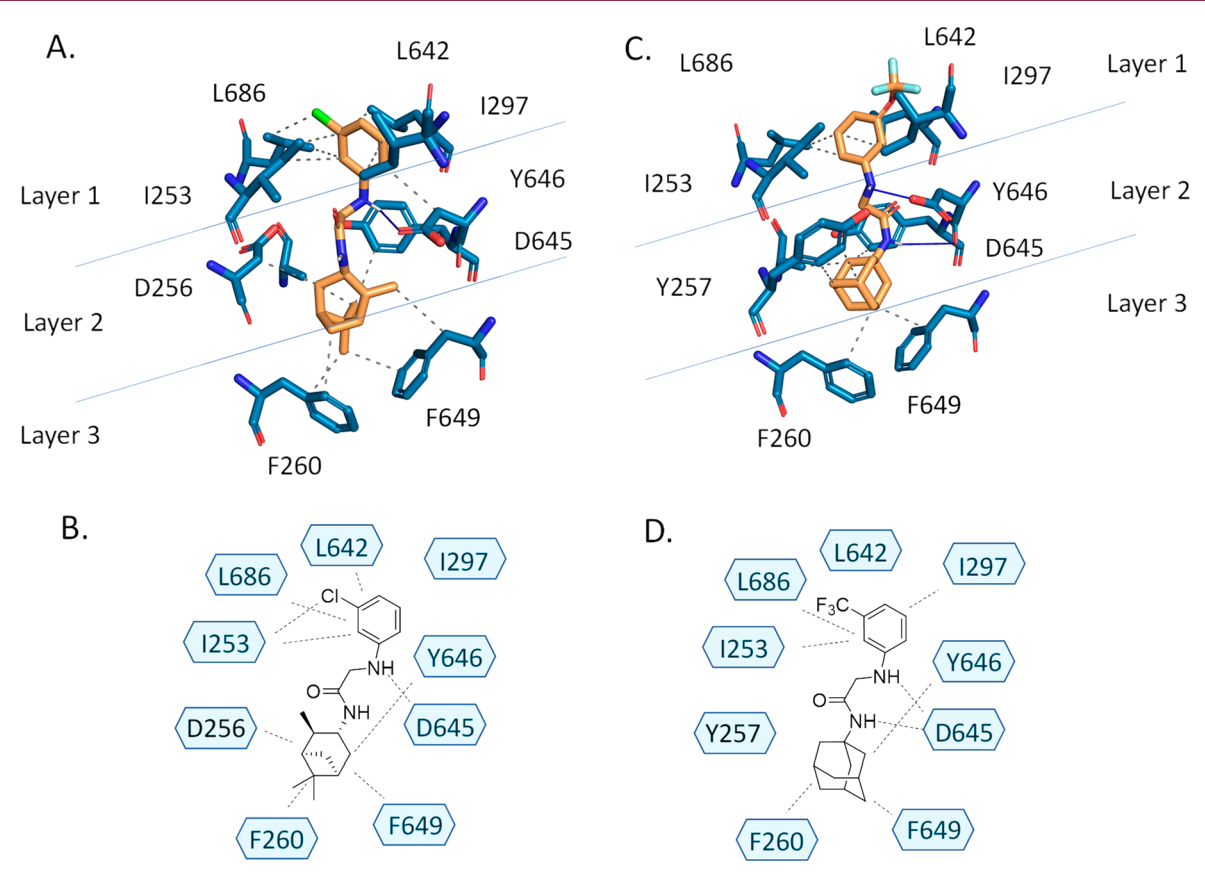


Figure 5. Stable docked complexes for lead acetamides 69 (panel A) and 76 (panel C). Panels B and D are orthogonal views of MmpL3-bound 69 and 76, respectively. Dotted lines indicate hydrophobic interactions, and solid blue lines indicate hydrogen bonding. Yellow = inhibitor carbon atoms, blue = nitrogen atoms, lime green = chlorine atom, red = oxygen atoms, green = MmpL3 amino acid residues' carbon atoms, light blue = fluorine atoms.

Ile253, Ile297, Leu642, and Leu686. Our modeling results with our novel acetamides, in concert with published MmpL3 crystal structures co-crystalized with SQ109, ICA38, and NITD-349, support a conserved binding site for this chemotype of MmpL3 inhibitors.

#### CONCLUSION

The structural changes made to the IC scaffold resulted in pyrrole-, mandelic acid-, imidazole-, and acetamide-based compounds with good ADME-Tox profiles. The top lead acetamides, 69 and 76, exhibited MIC values of 0.5  $\mu$ g/mL against M. abscessus and 0.25 µg/mL against M.tb. These inhibitors were found to be highly potent MmpL3 inhibitors. The aqueous solubility for the acetamide class improved up to 30-fold over the IC class, achieving nearly 30  $\mu$ g/mL. The permeability profiles of the compounds were moderate, and the HPPBs were generally high. This acetamide series of compounds were found to be very safe at all concentrations up to 20  $\mu$ g/mL, and the compounds achieved selectivity indices in the range of >10 to >80. Among the currently marketed first line anti-M.tb drugs, isoniazid and ethambutol have the lowest and the highest MIC values, respectively. The MIC for isoniazid is 0.02–0.08  $\mu$ g/mL, whereas for ethambutol it is 3– 5 µg/mL.34,35 Our mechanism of action studies suggest that lead acetamides 69 and 76 are MmpL3 inhibitors. Docking studies support a conserved binding site with known MmpL3 inhibitors. All in all, this series has a good drug disposition profile, as evidenced by favorable ADME data, making them

excellent candidates for further medicinal chemistry optimization to improve antimycobacterial activity.

#### **■ EXPERIMENTAL SECTION**

Methods and Instrumentation. All the reagents, glassware, solvents, and chemicals were purchased from commercially available sources. All the chemicals were reagent-grade and were used directly without further purification. The reactions were tracked and monitored by using fluorescent silica-gel-coated thin-layer chromatography (TLC) plates, and the spots were visualized using a UV lamp or iodine condensation. The purification of the compounds was performed using flash chromatography on a Biotage Isolera One with a Biotage silica gel column. <sup>1</sup>H and <sup>13</sup>C NMR spectra were recorded on a 400 MHz Bruker NMR system, and the chemical shifts were reported relative to the solvent peaks. Mass spectra were obtained on an Agilent 1200/AB Sciex API 5500 QTrap LC/MS/MS instrument using electrospray ionization and a single quadrupole analyzer (Q1). Analytical reverse-phase HPLC for acetamides was performed on Shimadzu's HPLC system equipped with a Kinetex C18 column (50  $\times$  3 mm; 5  $\mu$ m), flow rate of 0.5 mL/min, and a gradient of solvent A (water with 0.1% formic acid) and solvent B (acetonitrile): 0-1 min 5% B, 1-8 min 5% to 95% B, 8-9 min 95% B, 9-10 min 95% to 5% B. For all other compounds, chromatography was performed on an Agilent 1260 Infinity Quaternary LC system equipped with an Acquity BEH C18 column (1.7  $\mu$ m), flow rate of 1 mL/min, and a gradient of solvent A (water with 0.1% formic acid) and solvent B (acetonitrile with 0.1% formic acid): 0-2.5 min 20% A, 2.5-8.0 min 20% to 70% A (linear gradient), 8.0-9.0 min 70% to 20% A (linear gradient), 9-10 min 20% A. For purity determination of pyrrole- and histidine-based compounds, UV absorbance at 254 nm and 280 nm was used as the detection method, and 254 nm was used for all

acetamides. All pyrrole-, histidine-, and acetamide-based compounds were found to have a purity of >95% with the described analytical methods. Elemental analysis (CHN) was conducted on mandelic acid analogs due to their poor UV absorbance at 254 nm and 280 nm. Elemental analysis was performed by Galbraith Laboratories, Inc. (Knoxville, TN).

General Synthetic Method for Mandelic Acid, Pyrrole, and Imidazole Series. Aromatic carboxylic acid (1 equiv) was added to hydroxybenzotriazole (HOBT, 1 equiv), 1-ethyl-3-(3-(dimethylamino)propyl)carbodiimide (EDC, 1.2 equiv), and trimethylamine (TEA, 1.5 equiv) and stirred in dimethylformamide (DMF, 10 mL used per 100 mg of acid) for 15 min at room temperature. The bulky amine (1 equiv) was added to the reaction mixture and stirred under a  $N_2$  atmosphere overnight. The reaction mixture was diluted in water and extracted with ethyl acetate. The organic layer was removed and evaporated under reduced pressure. The crude product was purified using flash chromatography. For the mandelic acid analogs, the gradient used was 0–40% of ethyl acetate in hexane, whereas the PCs and imidazole-2-carboxamides eluted with a gradient of 25–55% of ethyl acetate in hexane.

4-(trans-Methyl)-cyclohexyl-pyrrole-2-carboxamide (5). 397 mg (96%) of off-white powder;  $^{1}$ H NMR (CDCl<sub>3</sub>)  $\delta$  = 0.91 (d, J = 6 Hz, 3H), 1.03–1.26 (m, 4H), 1.31–1.41 (m, 1H), 1.72–1.77 (m, 2H), 2.00–2.07 (m, 2H), 3.81–3.91 (m, 1H), 5.67 (s, 1H), 6.20–6.22 (m, 1H), 6.49–6.51 (m, J = 1 Hz, 1H), 6.89–6.91 (m, J = 1 Hz, 1H), 9.63 (s, 1H);  $^{13}$ C NMR (CDCl<sub>3</sub>)  $\delta$  = 22.20, 32.00, 33.43, 33.88, 48.37, 108.04, 109.74, 121.04, 160.21; ESI-MS calculated for  $C_{12}H_{19}N_2O$ : 207.2, found: 207.3 [M+H]<sup>+</sup>.

(1R,2R,3R,5S)-(-)-lsopinocampheyl-pyrrole-2-carboxamide (6). 370 mg (75%) of off-white powder;  $^{1}$ H NMR (CDCl<sub>3</sub>)  $\delta$  = 0.91 (d, J = 10 Hz, 1H), 1.09 (s, 3H), 1.15 (d, J = 7 Hz, 3H), 1.24 (s, 3H), 1.53–1.63 (m, 4H), 1.83–1.90 (m, 2H), 1.97–2.01 (m, 1H), 2.42–2.48 (m, 1H), 2.63–2.70 (m, 1H), 4.39–4.48 (m, 1H), 5.68–5.70 (m, 1H), 6.23–6.25 (m, 1H), 6.52–6.54 (m, J = 1 Hz, 1H), 6.91–6.93 (m, J = 1 Hz, 1H,);  $^{13}$ C NMR (CDCl<sub>3</sub>)  $\delta$  = 19.73, 22.37, 27.01, 34.38, 36.41, 37.43, 40.61, 45.55, 46.71, 46.79, 106.95, 108.74, 120.04, 159.39; ESI-MS calculated for C<sub>15</sub>H<sub>23</sub>N<sub>2</sub>O: 247.2, found: 247.1 [M +H]<sup>+</sup>.

*Cycloheptyl-pyrrole-2-carboxamide* (7). 155 mg (37.67%) of white powder;  $^{1}$ H NMR (CDCl<sub>3</sub>)  $\delta$  = 1.52–1.54 (m, 4H), 1.57 (s, 7H), 1.97–1.20 (m, 2H), 4.08–4.15 (m, 1H), 5.75 (s, 1H), 6.22–6.24 (m, 1H), 6.48–6.50 (sextet, J = 1 Hz, 1H), 6.89–6.91 (m, J = 1 Hz, 1H), 9.27 (s, 1H);  $^{13}$ C NMR (CDCl<sub>3</sub>)  $\delta$  = 24.12, 28.06, 35.37, 105.70, 109.78, 121.07, 159.91; ESI-MS calculated for  $C_{12}H_{19}N_2O$ : 207.2, found: 207.0 [M+H] $^+$ .

*Cyclooctyl-pyrrole-2-carboxamide* (8). 259 mg (58%) of white powder;  $^1$ H NMR (CDCl<sub>3</sub>)  $\delta$  = 1.54–1.73 (m, 12H), 1.87–1.94 (m, 2H), 3.49–3.50 (d, J = 5 Hz, 1H), 4.12–4.18 (m, 1H), 5.75–5.76 (m, 1H), 6.21–6.24 (d, J = 7 Hz, 1H,), 6.48–6.50 (t, J = 7 Hz, 1H), 6.89–6.91 (t, J = 5 Hz, 1H);  $^{13}$ C NMR (CDCl<sub>3</sub>)  $\delta$  = 23.68, 25.46, 27.34, 32.59, 49.34, 107.99, 109.78, 121.07, 159.91; ESI-MS calculated for C<sub>13</sub>H<sub>21</sub>N<sub>2</sub>O: 221.2, found: 221.2 [M+H] $^+$ .

1-Adamantyl-pyrrole-2-carboxamide (9). 317 mg (65%) of white powder,  $^1$ H NMR (CDCl<sub>3</sub>)  $\delta$  = 1.58 (s, 1H), 1.71 (s, 6H), 2.10 (s, 9H), 5.54 (s, 1H), 6.19–6.21 (m, 1H), 6.43–6.45 (m, J = 1 Hz, 1H), 6.87–6.89 (m, J = 1 Hz, 1H);  $^{13}$ C NMR (CDCl<sub>3</sub>)  $\delta$  = 29.52, 30.94, 36.38, 41.97, 52.06, 107.75, 109.63, 120.83, 160.25; ESI-MS calculated for C<sub>15</sub>H<sub>21</sub>N<sub>2</sub>O: 245.2, found: 245.2 [M+H] $^+$ .

2-Adamantyl-pyrrole-2-carboxamide (10). 297 mg (61%) of white powder,  ${}^{1}$ H NMR (CDCl<sub>3</sub>)  $\delta$  = 1.56 (s, 1H), 1.67 (s, 1H), 1.71 (s, 1H), 1.77 (s, 2H), 1.83 (s, 1H), 1.89 (s, 7H), 2.01 (s, 2H), 4.19–4.23 (m, 1H), 6.17 (s, 1H), 6.23–6.25 (m, 1H), 6.54–6.55 (m, 1H), 6.90–6.91 (m, J = 6 Hz, 1H);  ${}^{13}$ C NMR (CDCl<sub>3</sub>)  $\delta$  = 27.13, 27.25, 32.04, 32.14, 37.15, 37.54, 53.05, 109.76, 121.03, 160.01; ESI-MS calculated for C<sub>15</sub>H<sub>21</sub>N<sub>2</sub>O: 245.2, found: 245.2 [M+H] $^{+}$ .

*Geranyl-pyrrole-2-carboxamide* (11). 419 mg (85%) of off-white sticky powder; <sup>1</sup>H NMR (CDCl<sub>3</sub>-d)  $\delta$  = 1.61 (s, 3H), 1.68 (s, 3H), 1.71 (s, 3H), 2.00–2.17 (m, 4H), 4.04 (t, J = 6 Hz, 2H), 5.11 (t, J = 17 Hz, 1H), 5.29 (t, J = 17 Hz, 1H), 5.93 (s, 1H), 6.21 (d, J = 8 Hz, 1H), 6.54 (t, J = 7 Hz, 1H), 6.91 (t, J = 6 Hz, 1H); <sup>13</sup>C NMR

(CDCl<sub>3</sub>-d)  $\delta$  = 16.35, 17.73, 22.42, 23.41, 25.72, 26.41, 31.47, 32.01, 36.52, 37.15, 39.09, 108.71, 109.99, 111.46, 120.92, 121.61, 123.67, 126.02, 124.79, 128.64, 131.81, 132.21, 139.99, 140.14, 161.20; ESI-MS calculated for  $C_{15}H_{23}N_2O$ : 247.1, found: 247.1 [M+H]<sup>+</sup>.

4-(trans-Methyl)-cyclohexyl-imidazole-2-carboxamide (12). 364 mg (88%) of white powder  $^{1}$ H NMR (CDCl<sub>3</sub>)  $\delta$  = 0.91 (d, J = 7 Hz, 3H), 1.04–1.14 (m, 2H), 1.24–1.39 (m, 3H), 1.69–1.78 (m, 2H), 2.00–2.06 (m, 2H), 3.49–3.50 (m, 1H), 3.81–3.90 (m, J = 4 Hz, 1H), 7.11–7.16 (m, 2H);  $^{13}$ C NMR (CDCl<sub>3</sub>)  $\delta$  = 22.24, 31.86, 32.91, 33.95, 48.64, 118.75, 129.28, 141.51, 157.89; ESI-MS calculated for C<sub>11</sub>H<sub>18</sub>N<sub>3</sub>O: 208.1, found: 208.1 [M+H]<sup>+</sup>.

(18,2R,3R,5S)-(-)-Isopinocampheyl-imidazole-2-carboxamide (13). 440 mg (89%) of off-white powder;  $^{1}$ H NMR (CDCl<sub>3</sub>)  $\delta$  = 0.88–0.98 (m, 1H), 1.02 (s, 2H), 1.08 (d, J = 7 Hz, 2H), 1.18 (s, 2H), 1.65–1.71 (m, 1H), 1.78–1.82 (m, 1H), 1.91–1.95 (m, 1H), 1.97–2.02 (m, 1H), 2.34–2.41 (m, 1H), 2.52–2.59 (m, 1H), 4.34–4.42 (m, 1H), 7.12 (s, 1H), 7.19 (s, 2H);  $^{13}$ C NMR (CDCl<sub>3</sub>)  $\delta$  = 20.83, 23.45, 28.05, 35.12, 36.61, 38.54, 41.57, 45.54, 47.81, 48.04, 119.45, 129.30, 141.42, 158.52; ESI-MS calculated for C<sub>14</sub>H<sub>22</sub>N<sub>3</sub>O: 248.2, found: 248.2 [M+H]<sup>+</sup>.

2-Adamantyl-imidazole-2-carboxamide (14). 362 mg (74%) of white powder;  $^1$ H NMR (CDCl<sub>3</sub>)  $\delta$  = 1.19 (s, 1H), 1.49 (s, 6H), 1.65 (t, J = 3 Hz, 3H), 2.04–2.08 (m, 2H), 2.16 (m, 2H), 7.28–7.32 (m, 2H);  $^{13}$ C NMR (CDCl<sub>3</sub>-d)  $\delta$  = 27.11, 27.19, 31.83, 32.04, 37.14, 37.49, 53.47, 118.81, 129.69, 141.13, 157.45; ESI-MS calculated for C<sub>14</sub>H<sub>20</sub>N<sub>3</sub>O: 246.2, found: 246.1 [M+H]<sup>+</sup>.

*Cyclooctyl-imidazole-2-carboxamide* (15). 422 mg (96%) of offwhite powder;  $^{1}$ H NMR (CDCl<sub>3</sub>)  $\delta$  = 1.46–1.89 (m, 11H), 4.06–4.14 (m, J = 4 Hz, 1H), 7.15 (s, 1H), 7.19 (s, 2H);  $^{13}$ C NMR (CDCl<sub>3</sub>)  $\delta$  = 23.76, 25.49, 27.17, 31.87, 118.19, 127.21, 141.63, 151.71; ESI-MS calculated for  $C_{12}H_{20}N_3O$ : 222.2, found: 222.2 [M +H] $^{+}$ .

*Cycloheptyl-imidazole-2-carboxamide* (**16**). 397 mg (96%) of white powder;  $^{1}$ H NMR (CDCl<sub>3</sub>)  $\delta$  = 1.25 (s, 1H), 1.51–1.72 (m, 14H), 1.98–2.05 (m, 1H), 4.06–4.15 (m, 1H), 7.11–7.12 (m, 1H), 7.13–7.14 (m, 1H);  $^{13}$ C NMR (CDCl<sub>3</sub>)  $\delta$  = 24.12, 28.09, 30.96, 34.94, 50.74, 119.51, 129.11, 141.22, 157.23; ESI-MS calculated for  $C_{11}H_{18}N_3O$ : 208.1, found: 208.2 [M+H]<sup>+</sup>.

1-Adamantyl-imidazole-2-carboxamide (17). 365 mg (75%) of white powder;  $^{1}$ H NMR (CDCl<sub>3</sub>)  $\delta$  = 1.56 (s, 1H), 1.59 (s, 3H), 1.72 (s, 4H), 2.12 (s, 7H), 3.49 (d, J = 6 Hz, 1H), 7.09 (m, 1H), 7.11–7.13 (m, 1H);  $^{13}$ C NMR (CDCl<sub>3</sub>)  $\delta$  = 22.56, 29.45, 36.31, 41.55, 52.44, 119.27, 129.27, 141.94, 158.17; ESI-MS calculated for C<sub>14</sub>H<sub>20</sub>N<sub>3</sub>O: 246.2, found: 246.2 [M+H]<sup>+</sup>.

*Geranyl-imidazole-2-carboxamide* (18). 441 mg (89%) of yellow powder;  $^1$ H NMR (CDCl<sub>3</sub>-d)  $\delta$  = 1.60 (s, 3H), 1.63 (s, 3H), 1.68–1.69 (m, 3H), 1.72 (s, 3H), 2.00–2.12 (m, 4H), 3.49–3.50 (m, 1H), 4.04 (t, J = 6 Hz, 2H), 5.06–5.11 (m, 1H), 5.26–5.31 (m, 1H), 7.13 (t, J = 1 Hz, 1H), 7.15–7.16 (q, J = 1 Hz, 1H);  $^{13}$ C NMR (CDCl<sub>3</sub>-d)  $\delta$  = 16.36, 17.71, 25.69, 26.38, 37.18, 39.79, 118.79, 119.17, 123.80, 129.74, 131.86, 140.54, 141.25; ESI-MS calculated for C<sub>14</sub>H<sub>22</sub>N<sub>3</sub>O: 248.2, found: 248.2 [M+H]<sup>+</sup>.

trans-4-Methyl-cyclohexyl-2-phenyl-2-hydroxyl ethanamide (19). 469 mg (45%) of white powder;  $^1\text{H}$  NMR (CDCl<sub>3</sub>)  $\delta$  = 0.87 (d, J = 6 Hz, 3H), 0.95–1.15 (m, 5H), 1.23–1.33 (m, 1H), 1.35–1.71 (m, 2H), 1.85–1.93 (m, 2H), 3.62–3.71 (m, 1H), 3.78 (d, J = 4 Hz, 1H), 4.94 (d, J = 4 Hz, 1H), 5.97 (bs, 1H), 7.29–7.37 (m, 5H);  $^{13}\text{C}$  NMR (CDCl<sub>3</sub>)  $\delta$  = 14.13, 22.11, 22.66, 31.59, 32.96, 33.70, 48.72, 74.07, 126.88, 128.84, 139.70, 171.27; ESI-MS calculated for C<sub>15</sub>H<sub>21</sub>NO<sub>2</sub>Na: 270.2, found: 270.2 [M+Na]<sup>+</sup>. Elemental analysis calculated: C, 73.53; H, 8.87; N, 5.36; found: C, 72.85; H, 9.30; N, 5.70

(1R,2R,3R,5S)-(-)-lsopinocampheyl-2-phenyl-2-hydroxyl ethanamide (20). 93 mg (8%) of white powder;  $^{1}$ H NMR (CDCl<sub>3</sub>)  $\delta$  = 0.77–0.82 (m, 1H), 1.01–1.02 (m, 3H), 1.03 (s, 1H), 1.05 (s, 1H), 1.20 (s, 3H), 1.38–1.51 (m, 1H), 1.64–1.81 (m, 2H), 1.89–1.94 (m, 1H), 2.34–2.41 (m, 1H), 2.48–2.57 (m, 1H), 4.04 (s, 1H), 4.19–4.27 (m, 1H), 4.96 (s, 1H), 6.21–6.25 (m, 1H), 7.33–7.41 (m, 5H);  $^{13}$ C NMR (CDCl<sub>3</sub>)  $\delta$  = 20.71, 23.34, 28.01, 35.26, 36.77, 38.42, 41.53, 46.08, 47.68, 48.03, 74.13, 126.93, 128.89, 139.81, 171.42; ESI-

MS calculated for  $C_{18}H_{26}NO_2$ : 288.2, found: 288.3 [M+H]<sup>+</sup>. Elemental analysis calculated: C, 75.71; H, 9.03; N, 4.65; found: C, 74.33; H, 8.74; N, 4.12.

*Cycloheptyl-2-phenyl-2-hydroxyl ethanamide* (21). 789 mg (69%) of white powder; <sup>1</sup>H NMR (CDCl<sub>3</sub>)  $\delta$  = 1.30–1.61 (m, 12H), 1.79–1.92 (m, 2H), 2.88 (s, 2H), 2.95 (s, 2H), 3.63 (d, J = 4 Hz, 1H), 3.90–3.98 (m, J = 5 Hz, 1H), 4.98 (d, J = 4 Hz, 1H), 5.93–5.99 (m, 1H), 7.31–7.40 (m, 5H); <sup>13</sup>C NMR (CDCl<sub>3</sub>)  $\delta$  = 23.93, 24.02, 27.84, 31.45, 34.93, 34.94, 36.50, 50.71, 74.09, 126.88, 128.65, 128.92, 139.70, 162.55, 170.74; ESI-MS calculated for C<sub>15</sub>H<sub>21</sub>NO<sub>2</sub>Na: 270.2, found: 270.1 [M+Na]<sup>+</sup>. Elemental analysis calculated: C, 73.53; H, 8.87; N, 5.36; found: C, 73.25; H, 8.30; N, 5.64.

*Cyclooctyl-2-phenyl-2-hydroxyl ethanamide* (22). 178 mg (17%) of white powder;  $^1\text{H}$  NMR (CDCl<sub>3</sub>)  $\delta = 1.41 - 1.56$  (m, 13H), 1.69–1.81 (m, 2H), 3.55 (d, J = 4 Hz, 1H), 3.93–4.02 (m, J = 5 Hz, 1H), 4.97 (d, J = 4 Hz, 1H), 5.89–5.91 (m, 1H), 7.31–7.40 (m, 5H);  $^{13}\text{C}$  NMR (CDCl<sub>3</sub>)  $\delta = 23.56$ , 25.37, 27.12, 32.22, 49.73, 74.09, 126.88, 128.69, 128.96, 139.73, 170.67; ESI-MS calculated for C<sub>16</sub>H<sub>24</sub>NO<sub>2</sub>: 262.2, found: 262.1 [M+H] $^+$ . Elemental analysis calculated: C, 74.14; H, 9.15; N, 5.09; found: C, 73.82; H, 8.21; N, 5.19.

1-Adamantyl-2-phenyl-2-hydroxyl ethanamide (23). 534 mg (45%) of white powder;  $^{1}$ H NMR (CDCl<sub>3</sub>)  $\delta$  = 1.58 (s, 6H), 1.86–1.87 (m, 6H), 1.99 (s, 3H), 3.63 (bs, 1H), 4.81 (s, 1H), 5.55 (s, 1H), 7.24–7.31 (m, 5H);  $^{13}$ C NMR (CDCl<sub>3</sub>)  $\delta$  = 29.37, 36.22, 41.43, 52.24, 74.09, 126.88, 128.59, 128.92, 140.00, 171.02; ESI-MS calculated for C<sub>18</sub>H<sub>23</sub>NO<sub>2</sub>Na: 308.2, found: 308.0 [M+Na]<sup>+</sup>. Elemental analysis calculated: C, 76.22; H, 8.42; N, 4.68; found: C, 75.12; H, 7.53; N, 4.53.

2-Adamantyl-2-phenyl-2-hydroxy ethanamide (24). 701 mg (62%) of white powder;  $^1$ H NMR (CDCl<sub>3</sub>)  $\delta$  = 1.42–1.46 (m, 1H), 1.55–1.56 (m, 1H), 1.59 (s, 1H), 1.61–1.63 (m, 2H), 1.70–1.71 (m, 2H), 1.76–1.89 (m, 8H), 3.48–3.49 (m, 2H), 3.65 (d, J = 3 Hz, 1H), 4.01–4.05 (m, 1H), 5.04 (d, J = 3 Hz, 1H), 6.34 (bs, 1H), 7.32–7.43 (m, 5H);  $^{13}$ C NMR (CDCl<sub>3</sub>)  $\delta$  = 14.21, 21.07, 26.98, 27.06, 31.77, 31.84, 36.92, 37.01, 37.40, 53.45, 60.42, 126.76, 128.69, 139.81, 170.13; ESI-MS calculated for C<sub>18</sub>H<sub>24</sub>NO<sub>2</sub>: 286.2, found: 286.0 [M+H] $^+$ . Elemental analysis calculated: C, 76.22; H, 8.42; N, 4.68; found: C, 76.20; H, 7.97; N, 4.97.

trans-4-Methyl-cyclohexyl-2S-phenyl-2-hydroxyl ethanamide (25). 373 mg (25%) of off-white powder;  $^1$ H NMR (CDCl<sub>3</sub>)  $\delta$  = 0.79–0.82 (m, 3H), 0.90–1.09 (m, 4H), 1.18–1.27 (m, 1H), 1.58–1.65 (m, 2H), 1.78–1.89 (m, 2H), 3.37–3.67 (m, 2H), 4.91 (s, 1H), 5.75 (bs, 1H), 7.24–7.37 (m, 5H);  $^{13}$ C NMR (CDCl<sub>3</sub>)  $\delta$  = 22.12, 31.85, 32.99, 33.71, 48.79, 74.09, 126.93, 129.26, 139.65, 171.18; ESI-MS calculated for C<sub>15</sub>H<sub>22</sub>NO<sub>2</sub>: 248.2, found: 248.2 [M+H]<sup>+</sup>. Elemental analysis calculated: C, 73.53; H, 8.87; N, 5.36; found: C, 73.06; H, 7.53; N, 5.18.

(1R,2R,3R,5S)-(-)-lsopinocampheyl-2-phenyl-2S-hydroxyl ethanamide (26). 537 mg (31%) of white powder; <sup>1</sup>H NMR (CDCl<sub>3</sub>)  $\delta$  = 0.80 (d, J = 10 Hz, 1H), 1.04 (s, 3H), 1.07 (d, J = 7 Hz, 2H), 1.23 (s, 3H), 1.39–1.45 (m, 1H), 1.74–1.83 (m, 2H), 1.91–1.96 (m, 1H), 2.36–2.43 (m, 1H), 2.52–2.59 (m, 1H), 3.94 (s, 1H), 4.22–4.30 (m, 1H), 4.99 (s, 1H), 6.18–6.20 (m, 1H), 7.33–7.41 (m, 5H); <sup>13</sup>C NMR (CDCl<sub>3</sub>)  $\delta$  = 20.71, 23.34, 28.01, 35.26, 36.77, 38.42, 41.53, 46.08, 47.68, 48.03, 74.13, 126.93, 128.89, 139.81, 171.42; ESI-MS calculated for C<sub>18</sub>H<sub>26</sub>NO<sub>2</sub>: 288.2, found: 288.2 [M+H]<sup>+</sup>. Elemental analysis calculated: C, 75.71; H, 9.03; N, 4.65; found: C, 75.31; H, 9.09; N, 4.84.

*Cycloheptyl-2-phenyl-2S-hydroxyl ethanamide (27).* 366 mg (21%) of white powder;  $^{1}$ H NMR (CDCl<sub>3</sub>)  $\delta$  = 1.26–1.57 (m, 11H), 1.75–1.83 (m, 2H), 3.78–3.87 (m, J = 4 Hz, 1H), 4.50 (s, 1H), 4.84 (s, 1H), 6.54 (bs, 1H), 7.27–7.34 (m, 5H);  $^{13}$ C NMR (CDCl<sub>3</sub>)  $\delta$  = 23.99, 27.89, 34.82, 50.36, 73.98, 126.74, 125.31, 128.59, 139.98, 171.21; ESI-MS: calculated for  $C_{15}H_{22}NO_2$ : 248.2, found: 248.2 [M+H]<sup>+</sup>. Elemental analysis calculated: C, 73.53; H, 8.87; N, 5.36; found: C, 73.11; H, 7.85; N, 5.52.

*Cyclooctyl-2-phenyl-2S-hydroxyl ethanamide* (**28**). 426 mg (27%) of transparent oily liquid;  $^1H$  NMR (CDCl<sub>3</sub>)  $\delta = 1.38-1.74$  (m, 12H), 3.82-3.91 (m, 1H), 4.83-4.86 (m, 2H), 6.74-6.76 (m, 1H), 7.24-7.47 (m, 5H);  $^{13}$ C NMR (CDCl<sub>3</sub>)  $\delta = 23.56$ , 25.35, 27.11,

32.19, 49.70, 60.43, 74.07, 126.88, 127.46, 128.84, 139.69, 170.30; ESI-MS calculated for  $C_{16}H_{24}NO_2$ : 262.2, found: 262.1 [M+H]<sup>+</sup>. Elemental analysis calculated: C, 74.14; H, 9.15; N, 5.09; found: C, 73.21; H, 8.93; N, 5.27.

1-Adamantyl-2-phenyl-2S-hydroxyl ethanamide (29). 446 mg (26%) of white powder;  $^{1}$ H NMR (CDCl<sub>3</sub>)  $\delta$  = 1.64 (s, 6H), 1.92—1.93 (m, 6H), 2.04 (s, 3H), 4.12 (s, 1H), 4.81 (s, 1H), 5.94 (s, 1H), 7.30—7.36 (m, 5H);  $^{13}$ C NMR (CDCl<sub>3</sub>)  $\delta$  = 29.39, 36.26, 41.42, 52.09, 74.12, 126.84, 128.39, 128.76, 140.11, 171.23; ESI-MS calculated for C<sub>18</sub>H<sub>24</sub>NO<sub>2</sub>: 286.2, found: 286.0 [M+H]<sup>+</sup>. Elemental analysis calculated: C, 76.22; H, 8.42; N, 4.68; found: C, 70.19; H, 6.87; N, 3.37.

2-Adamantyl-2-phenyl-2S-hydroxyl ethanamide (30). 308 mg (18%) of white powder;  $^1\text{H}$  NMR (CDCl $_3$ )  $\delta=0.87-1.91$  (m, 10H), 3.78-3.93 (m, 1H), 5.23-5.40 (m, 1H), 6.04-6.19 (m, 1H), 7.28-7.44 (m, 5H);  $^{13}\text{C}$  NMR (CDCl $_3$ )  $\delta=26.89$ , 31.57, 36.92, 37.34, 53.11, 73.28, 126.88, 127.48, 128.84, 129.13, 135.36, 137.81, 165.56, 171.80; ESI-MS calculated for C $_{18}\text{H}_{24}\text{NO}_2$ : 286.2, found: 286.1 [M +H] $^+$ . Elemental analysis calculated: C, 76.22; H, 8.42; N, 4.68; found: C, 73.31; H, 7.86; N, 4.08.

trans-4-Methyl-cyclohexyl-2-phenyl-2R-hydroxyl ethanamide (31). 341 mg (23%) of white powder;  $^1\text{H}$  NMR (CDCl<sub>3</sub>)  $\delta$  = 0.89 (d, J = 7 Hz, 3H), 0.99–1.85 (m, 4H), 1.26–1.36 (m, 1H), 1.67–1.74 (m, 2H), 1.87–1.97 (m, 2H), 3.67–3.77 (m, 1H), 5.00 (s, 1H), 5.80–5.82 (m, 1H), 7.36–7.42 (m, 5H);  $^{13}\text{C}$  NMR (CDCl<sub>3</sub>)  $\delta$  = 22.19, 31.85, 32.89, 33.72, 73.99, 126.81, 128.31, 128.63, 139.89, 171.65; ESI-MS calculated for C<sub>15</sub>H<sub>22</sub>NO<sub>2</sub>: 248.2, found: 248.2 [M +H] $^+$ . Elemental analysis calculated: C, 73.53; H, 8.87; N, 5.36; found: C, 72.49; H, 8.91; N, 5.51.

(1R,2R,3R,5S)-(-)-IsopinocampheyI-2-phenyI-2R-hydroxyI ethanamide (32). 717 mg (42%) of oily liquid;  $^1$ H NMR (CDCl<sub>3</sub>)  $\delta$  = 0.72 (d, J = 10 Hz, 1H), 0.95–0.97 (m, SH), 1.14 (s, 3H), 1.17–1.21 (t, J = 7 Hz, 1H), 1.39–1.45 (m, 1H), 1.53–1.61 (quintet, J = 8 Hz, 1H), 1.71 (t, J = 6 Hz, 1H), 1.85–1.89 (m, 1H), 2.29–2.35 (m, 1H), 2.46–2.53 (m, 1H), 4.16–4.24 (m, 1H), 4.94 (s, 1H), 5.85 (bs, 1H), 7.24–7.35 (m, SH);  $^{13}$ C NMR (CDCl<sub>3</sub>)  $\delta$  = 14.21, 21.08, 23.33, 27.99, 35.29, 36.92, 38.39, 41.48, 46.24, 48.12, 60.4341, 74.09, 126.87, 128.91, 139.73, 171.44; ESI-MS calculated for C<sub>18</sub>H<sub>26</sub>NO<sub>2</sub>: 288.2, found: 288.1 [M+H]<sup>+</sup>. Elemental analysis calculated: C, 75.71; H, 9.03; N, 4.65; found: C, 74.46; H, 8.91; N, 4.70.

*Cycloheptyl-2-phenyl-2R-hydroxyl ethanamide* (33). 368 mg (21%) of white powder; <sup>1</sup>H NMR (CDCl<sub>3</sub>)  $\delta$  = 0.74–1.04 (m, 1H), 1.19 (s, 1H), 1.23–1.52 (m, 10H), 1.72–1.84 (m, 2H), 3.41–3.69 (m, 1H), 3.83–3.92 (m, J = 5 Hz, 1H), 4.91 (s, 1H), 5.85–5.92 (m, 1H), 7.24–7.47 (m, 5H); <sup>13</sup>C NMR (CDCl<sub>3</sub>)  $\delta$  = 24.02, 27.83, 34.94, 50.72, 74.08, 126.89, 129.25, 139.67, 170.73; ESI-MS calculated for C<sub>15</sub>H<sub>22</sub>NO<sub>2</sub>: 248.2, found: 248.2 [M+H]<sup>+</sup>. Elemental analysis calculated: C, 73.53; H, 8.87; N, 5.36; found: C, 72.91; H, 7.94; N, 5.26.

*Cyclooctyl-2-phenyl-2R-hydroxyl ethanamide* (**34**). 643 mg (41%) of white powder; <sup>1</sup>H NMR (CDCl<sub>3</sub>)  $\delta$  = 1.18–1.75 (m, 14H), 3.87–3.95 (m, J = 4 Hz, 1H), 4.91 (s, 1H), 5.87 (bs, 1H), 7.24–7.46 (m, 5H); <sup>13</sup>C NMR (CDCl<sub>3</sub>)  $\delta$  = 23.55, 25.35, 27.11, 32.19, 49.71, 74.07 126.74, 128.93, 139.69, 170.71; ESI-MS calculated for C<sub>16</sub>H<sub>24</sub>NO<sub>2</sub>: 262.2, found: 262.2 [M+H]<sup>+</sup>. Elemental analysis calculated: C, 74.14; H, 9.15; N, 5.09; found: C, 73.69; H, 8.42; N, 5.12.

1-Adamantyl-2-phenyl-2R-hydroxyl ethanamide (35). 281 mg (16%) of white powder;  $^1$ H NMR (CDCl $_3$ )  $\delta$  = 1.64 (s, 6H), 1.93 (s, 6H), 2.03–2.05 (m, 3H), 3.99 (s, 1H), 4.83 (s, 1H), 5.84 (s, 1H), 7.29–7.36 (m, 5H);  $^{13}$ C NMR (CDCl $_3$ )  $\delta$  = 29.39, 36.29, 41.62, 52.28, 74.13, 126.81, 128.45, 128.63, 140.07, 171.29; ESI-MS calculated for C $_{18}$ H $_{24}$ NO $_2$ : 286.2, found: 286.1 [M+H] $^+$ . Elemental analysis calculated: C, 76.22; H, 8.42; N, 4.68; found: C, 75.67; H, 8.34; N, 4.80.

2-Adamantyl-2-phenyl-2R-hydroxy ethanamide (36). 501 mg (30%) of white powder;  $^{1}$ H NMR (CDCl<sub>3</sub>)  $\delta$  = 1.17–1.82 (m, 14H), 3.94–3.97 (m, 1H), 4.97 (s, 1H), 6.29 (bs, 1H), 7.24–7.44 (m, 5H);  $^{13}$ C NMR (CDCl<sub>3</sub>)  $\delta$  = 27.05, 31.76, 37.00, 53.44, 74.16, 127.47, 128.97, 139.79, 171.09; ESI-MS calculated for C<sub>18</sub>H<sub>24</sub>NO<sub>2</sub>: 286.2,

found: 286.1 [M+H]<sup>+</sup>. Elemental analysis calculated: C, 76.22; H, 8.42; N, 4.68; found: C, 75.89; H, 7.35; N, 4.61.

General Procedure for the Preparation of N-(Cycloalkyl)-2-(N-phenylamino)acetamides. TEA (1.2 equiv) was added to a solution of 1 equiv of aliphatic cycloalkylamine dissolved in anhydrous DCM and allowed to stir for 15 min at 0 °C under N<sub>2</sub> atmosphere. Bromoacetyl bromide (1.2 equiv) was added dropwise to the mixture, and the reaction was carried out for 4 h. The completion of the reaction was monitored by the derivatization of the spot by spraying H<sub>2</sub>SO<sub>4</sub>/ethanol solution followed by charring or by the iodine condensation method. The crude mixture was extracted twice with DCM. The DCM layer was collected, dried with anhydrous sodium sulfate (Na<sub>2</sub>SO<sub>4</sub>), and evaporated under a reduced pressure. Without purification, the crude product was dissolved in anhydrous THF, and TEA (1.2 equiv) and aniline analogs (1 equiv) were added. The reaction was carried out at 60 °C overnight. The completion of the reaction was monitored by spotting the crude in a TLC plate and observed using a UV lamp. The crude mixture was extracted twice with ethyl acetate, collected, dried with anhydrous Na2SO4, concentrated under reduced pressure, and adsorbed in silica. The crude product was purified using flash chromatography with an ethyl acetate-hexane solvent system, and the gradient was determined with the help of TLC, yielding the pure acetamides.

*N*-(*Cyclooctyl*)-2-(*N*-phenylamino)acetamide (**37**). 718 mg (70.0%) of pale yellow powder;  $^{1}$ H NMR (CDCl<sub>3</sub>)  $\delta$  = 1.29–1.79 (14H, m), 3.78 (2H, s), 4.07 (1H, s), 6.63 (2H, d, J = 8 Hz), 6.84 (1H, t, J = 8 Hz), 7.24 (2H, t, J = 8 Hz);  $^{13}$ C NMR (CDCl<sub>3</sub>)  $\delta$  = 23.55, 25.29, 27.15, 32.17, 49.12, 113.38, 119.19, 129.42, 147.23, 168.92; ESI-MS [M+H]<sup>+</sup> calculated for C<sub>16</sub>H<sub>24</sub>N<sub>2</sub>O: 261.2, found: 261.4

*N*-(*Cycloheptyl*)-2-(*N*-phenylamino)acetamide (**38**). 739 mg (68.0%) of pale yellow powder;  $^{1}$ H NMR (CDCl<sub>3</sub>)  $\delta$  = 1.36–1.61 (11H, m), 1.85–1.92 (2H, m), 3.79 (2H, s), 6.67 (2H, d, J = 8 Hz), 6.86 (1H, t, J = 8 Hz), 7.25 (2H, t, J = 8 Hz);  $^{13}$ C NMR (CDCl<sub>3</sub>)  $\delta$  = 24.01, 27.87, 35.02, 49.39, 50.20, 113.73, 119.61, 129.46, 146.8, 168.75; ESI-MS [M+H]<sup>+</sup> calculated for C<sub>15</sub>H<sub>22</sub>N<sub>2</sub>O: 247.2, found: 247.5.

*N*-(trans-Methylcyclohexyl)-2-(*N*-phenylamino)acetamide (*39*). 426 mg (49%) of white powder;  $^1$ H NMR (CDCl<sub>3</sub>)  $\delta$  = 0.89 (2H, d, J = 4 Hz), 1.03–1.13 (4H, m), 1.68–1.71 (2H, m), 1.91–1.93 (2H, m), 3.72–3.80 (1H, m), 3.83 (2H, s), 6.75 (2H, d, J = 8 Hz), 6.92 (1H, t, J = 8 Hz), 7.26 (2H, t, J = 4 Hz);  $^{13}$ C NMR (CDCl<sub>3</sub>)  $\delta$  = 22.14, 31.85, 33.00, 33.76, 48.20, 49.21, 113.35, 119.19, 129.42, 148.0, 169.0; ESI-MS [M+H]<sup>+</sup> calculated for C<sub>15</sub>H<sub>22</sub>N<sub>2</sub>O: 247.2, found:

*N*-(1*R*,2*R*,3*R*,5*S*)-(–)-*Isopinocampheyl*-2-(*N*-*phenylamino*)-*acetamide* (*40*). 364 mg (65%) of pale yellow powder; <sup>1</sup>H NMR (CDCl<sub>3</sub>)  $\delta$  = 0.76–0.79 (1H, m), 1.07–1.10 (6H, m), 1.12 (3H, s), 1.45–1.50 (1H, m), 1.68–1.72 (1H, m), 1.78–1.81 (1H, m), 1.91–1.95 (1H, m), 2.34–2.38 (1H, m), 2.56–2.63 (1H, m), 3.81 (2H, s), 4.30–4.38 (1H, m), 6.59 (1H, d, *J* = 8 Hz), 6.66 (2H, d, *J* = 8 Hz), 6.83 (1H, t, *J* = 8 Hz), 7.23 (2H, t, *J* = 8 Hz), <sup>13</sup>C NMR (CDCl<sub>3</sub>)  $\delta$  = 20.67, 23.37, 28.01, 35.24, 36.93, 38.40, 41.52, 46.08, 47.70, 49.19, 113.35, 119.14, 129.41, 147.30, 169.67; ESI-MS [M+H]<sup>+</sup> calculated for C<sub>18</sub>H<sub>26</sub>N<sub>2</sub>O: 287.2, found: 287.4.

*N*-(1-Adamantyl)-2-(*N*-phenylamino)acetamide (41). 168 mg (60%) of pale yellow powder; <sup>1</sup>H NMR (CDCl<sub>3</sub>)  $\delta$  = 1.59 (6H, s), 1.90 (6H, s), 1.99 (3H, s), 3.60 (2H, s), 6.31 (1H, s), 6.57 (2H, d, *J* = 8 Hz), 6.76 (1H, t, *J* = 8 Hz), 7.15 (2H, t, *J* = 8 Hz), <sup>13</sup>C NMR (CDCl<sub>3</sub>)  $\delta$  = 29.39, 36.29, 41.49, 45.25, 49.78, 51.63, 113.41, 119.08, 129.38, 147.29, 169.26; ESI-MS [M+H]<sup>+</sup> calculated for C<sub>18</sub>H<sub>24</sub>N<sub>2</sub>O: 285.2, found: 285.3.

*N*-(2-Adamantyl)-2-(*N*-phenylamino)acetamide (**42**). 675.73 mg (72%) of amber oil; <sup>1</sup>H NMR (CDCl<sub>3</sub>)  $\delta$  = 1.54 (4H, s), 1.62–1.67 (3H, m), 1.75–1.80 (8H, m), 3.83 (2H, s), 6.75 (2H, d, J = 8 Hz), 6.86 (1H, t, *J* = 8 Hz); 7.18 (2H, t, *J* = 8 Hz); <sup>13</sup>C NMR (CDCl<sub>3</sub>)  $\delta$  = 27.05, 31.76, 32.0, 37.07, 37.46, 49.42, 52.84, 113.55, 119.44, 129.45, 136.68, 153.72, 169.18; ESI-MS [M+H]<sup>+</sup> calculated for C<sub>18</sub>H<sub>24</sub>N<sub>2</sub>O: 285.2, found: 285.2.

*N*-(1*R*,2*R*,3*R*,5*S*)-(–)-Isopinocampheyl-2-(*N*-4′-chlorophenyl-amino)acetamide (*43*). 638 mg (61%) of amber oil; <sup>1</sup>H NMR (CDCl<sub>3</sub>)  $\delta$  = 0.74–0.76 (1H, m), 1.05–1.08 (6H, m), 1.21 (3H, d, J = 4 Hz), 1.40–1.46 (1H, m), 1.65–1.69 (1H, m), 1.77–1.80 (1H, m), 1.91–1.93 (1H, m), 2.36–2.38 (1H, m), 2.55–2.61 (1H, m), 3.76 (2H, s), 4.25–4.33 (1H, s), 6.54 (2H, d, J = 8 Hz), 7.15 (2H, d, J = 8 Hz); <sup>13</sup>C NMR (CDCl<sub>3</sub>)  $\delta$  = 20.67, 23.36, 27.98, 35.27, 36.93, 38.39, 41.48, 46.11, 47.65, 49.15, 62.16, 114.13, 114.69, 129.30, 169.08; ESI-MS [M+H]<sup>+</sup> calculated for C<sub>18</sub>H<sub>25</sub>ClN<sub>2</sub>O: 321.2, found:

*N*-(1*R*,2*R*,3*R*,55)-(−)-lsopinocampheyl-2-(*N*-4'-bromophenyl-amino)acetamide (44). 678 mg (57%) of amber oil; <sup>1</sup>H NMR (CDCl<sub>3</sub>)  $\delta$  = 0.67−0.69 (1H, m), 0.98−1.01 (6H, m), 1.14 (3H, s), 1.33−1.39 (1H, m), 1.58−1.62 (1H, m), 1.70−1.73 (1H, m), 1.83−1.86 (1H, m) 2.28−2.31 (1H, m), 2.47−2.54 (1H, m), 3.69 (2H, s), 4.20−4.28 (1H, m), 6.43 (2H, d, J = 8 Hz), 7.22 (2H, d, J = 8 Hz); <sup>13</sup>C NMR (CDCl<sub>3</sub>)  $\delta$  = 20.69, 23.38, 28.00, 35.31, 37.01, 38.39, 41.48, 46.19, 47.65, 48.96, 110.99, 114.27, 114.89, 132.17, 132.35, 146.22, 169.00; ESI-MS [M+H]<sup>+</sup> calculated for C<sub>18</sub>H<sub>25</sub>BrN<sub>2</sub>O: 365.1, found: 365.4.

*N*-(1*R*,2*R*,3*R*,55)-(–)-Isopinocampheyl-2-(*N*-4'-methylphenyl-amino)acetamide (*45*). 499 mg (51%) of amber oil; <sup>1</sup>H NMR (CDCl<sub>3</sub>)  $\delta$  = 0.75–0.77 (1H, m), 1.05–1.08 (6H, m), 1.20 (3H, s), 1.42–1.48 (1H, m), 1.57 (3H, s) 1.66–1.70 (1H, m), 1.77–1.79 (1H, m), 1.90–1.94 (1H, m), 2.33–2.37 (1H, m), 2.55–2.61 (1H, m), 3.75 (2H, s), 4.30–4.36 (1H, m), 6.53 (2H, d, *J* = 8 Hz), 7.01 (2H, d, *J* = 8 Hz); <sup>13</sup>C NMR (CDCl<sub>3</sub>)  $\delta$  = 20.68, 23.38, 28.02, 35.26, 36.95, 38.41, 41.54, 46.11, 47.41, 47.72, 49.62, 113.44, 128.50, 129.9, 145.05, 169.82; ESI-MS [M+H]<sup>+</sup> calculated for C<sub>19</sub>H<sub>28</sub>N<sub>2</sub>O: 301.2, found: 301.5

N-(1R,2R,3R,5S)-(-)-ls opinocampheyl-2-(N-4'-methoxyphenylamino) acetamide (46). 443 mg (43%) of dark amber oil;  $^1H$  NMR (CDCl<sub>3</sub>)  $\delta=0.75-0.77$  (1H, m), 1.05-1.08 (6H, m), 1.20 (3H, s), 1.42-1.48 (1H, m), 1.68-1.70 (1H, m), 1.76-1.79 (1H, m), 1.90-1.93 (1H, m), 2.34-2.37 (1H, m), 2.54-2.61 (1H, m), 3.73 (2H, s), 3.75 (3H, s), 4.29-4.34 (1H, m), 6.57 (2H, d, J=8 Hz), 6.79 (2H, d, J=8 Hz);  $^{13}$ C NMR (CDCl<sub>3</sub>)  $\delta=20.69, 23.38, 28.02, 35.26, 36.97, 38.40, 41.53, 46.14, 47.39, 47.71, 50.01, 55.74, 114.51, 114.94, 141.33, 153.20, 169.86; ESI-MS [M+H]+ calculated for C<sub>19</sub>H<sub>28</sub>N<sub>2</sub>O<sub>2</sub>: 317.2, found: 317.5.$ 

*N*-(1*R*,2*R*,3*R*,5*S*)-(-)-lsopinocampheyl-2-(*N*-4'-trifluoromethoxyphenylamino)acetamide (47). 384 mg (32%) of amber oil; <sup>1</sup>H NMR (CDCl<sub>3</sub>)  $\delta$  = 0.76 (1H, d, J = 12 Hz), 1.04–1.08 (6H, m), 1.21–1.27 (3H, m), 1.46–1.49 (1H, m), 1.68–1.71 (1H, m), 1.91–1.94 (1H, m), 2.36–2.39 (1H, m), 3.78 (2H, s), 4.30–4.34 (1H, m), 6.51 (1H, s), 6.59 (2H, d, J = 8 Hz), 7.06 (2H, d, J = 8 Hz); <sup>13</sup>C NMR (CDCl<sub>3</sub>)  $\delta$  = 20.65, 23.34, 27.96, 35.23, 36.96, 38.38, 41.48, 46.09, 47.65, 49.03, 113.70, 112.52, 141.60, 146.09, 169.19; C<sub>19</sub>H<sub>25</sub>F<sub>3</sub>N<sub>2</sub>O<sub>2</sub> ESI-MS [M+H]<sup>+</sup> calculated for C<sub>19</sub>H<sub>25</sub>F<sub>3</sub>N<sub>2</sub>O<sub>2</sub>: 370.2, found: 370.7.

*N-*(1*R*,2*R*,3*R*,5*S*)-(–)-*IsopinocampheyI-2-(N-4'-trifluoromethylphenylamino)acetamide* (*48*). 471 mg (41%) of amber oil; <sup>1</sup>H NMR (CDCl<sub>3</sub>)  $\delta$  = 0.67 (1H, d, J = 8 Hz), 0.97–1.01 (6H, m), 1.14 (3H, s), 1.35–1.40 (1H, m), 1.59–1.63 (1H, m), 1.70–1.73 (1H, m), 1.84–1.88 (1H, m), 2.27–2.33 (1H, m), 2.48–2.55 (1H, m), 3.75 (2H, s), 4.23–4.28 (1H, m), 6.22 (1H, s), 6.57 (2H, d, J = 8 Hz), 7.36 (2H, d, J = 8 Hz); <sup>13</sup>C NMR (CDCl<sub>3</sub>)  $\delta$  = 20.67, 23.35, 27.96, 35.27, 36.99, 38.38, 41.46, 46.19, 47.63, 47.75, 48.27, 112.58, 126.70, 126.77, 149.80, 168.69; ESI-MS [M+Na]<sup>+</sup> calculated for  $C_{19}H_{25}F_3N_2O$ : 377.2, found: 377.2.

N-(1-Adamantyl)-2-(N-4'-chlorophenylamino)acetamide (49). 286 mg (30%) of white powder;  $^1$ H NMR (CDCl<sub>3</sub>)  $\delta$  = 1.69 (6H, s), 1.98 (6H, s), 2.09 (3H, s), 3.66 (2H, s), 6.23 (1H, s), 6.56 (2H, d, J = 8 Hz), 7.17 (2H, d, J = 8 Hz);  $^{13}$ C NMR (CDCl<sub>3</sub>)  $\delta$  = 29.38, 36.26, 41.51, 49.54, 51.78, 114.43, 123.74, 129.25, 145.79, 168.69; ESI-MS [M+H] $^+$  calculated for C<sub>18</sub>H<sub>23</sub>ClN<sub>2</sub>O: 319.1, found: 319.1.

*N-*(1-Adamantyl)-2-(*N-*4'-bromophenylamino)acetamide (*50*). 283 mg (26%) of pale yellow powder; <sup>1</sup>H NMR (CDCl<sub>3</sub>)  $\delta$  = 1.68 (6H, s), 1.98 (6H, s), 2.08 (3H, s), 3.64 (2H, s), 6.50 (2H, d, J = 8 Hz), 7.29 (2H, d, J = 8 Hz); <sup>13</sup>C NMR (CDCl<sub>3</sub>)  $\delta$  = 29.37, 36.25,

41.51, 49.43, 51.78, 110.80, 114.91, 132.11, 146.24, 168.67; ESI-MS  $[M+H]^+$  calculated for  $C_{18}H_{23}BrN_2O$ : 363.1, found: 363.2.

*N*-(1-Adamantyl)-2-(*N*-4'-methylphenylamino)acetamide (*51*). 259 mg (29%) of white powder;  $^1$ H NMR (CDCl<sub>3</sub>)  $\delta$  = 1.68 (6H, s), 2.00 (6H, s), 2.08 (3H, s), 2.29 (3H, s), 3.67 (2H, s), 6.52 (1H, s) 6.60 (2H, d, *J* = 8 Hz), 7.04 (2H, d, *J* = 8 Hz);  $^{13}$ C NMR (CDCl<sub>3</sub>)  $\delta$  = 29.39, 36.29, 41,47, 50.34, 51.61, 113.83, 128.78. 129.88, 144.63, 169.29; ESI-MS [M+H]<sup>+</sup> calculated for C<sub>19</sub>H<sub>26</sub>N<sub>2</sub>O: 299.2, found: 299.4.

*N*-(1-Adamantyl)-2-(*N*-4'-methoxyphenylamino)acetamide (**52**). 292 mg (31%) of dark amber oil; <sup>1</sup>H NMR (CDCl<sub>3</sub>)  $\delta$  = 1.68 (6H, s), 2.0 (6H. s), 2.08 (3H, s), 3.65 (2H, s), 3.78 (3H, s), 6.57 (1H, s), 6.63 (2H, d, *J* = 8 Hz), 6.81 (2H, d, *J* = 8 Hz); <sup>13</sup>C NMR (CDCl<sub>3</sub>)  $\delta$  = 29.39, 36.39, 41.48, 50.8, 51.63, 55.72, 114.91, 115.03, 140.72, 153.48, 169.30; ESI-MS [M+H]<sup>+</sup> calculated for C<sub>19</sub>H<sub>26</sub>N<sub>2</sub>O<sub>2</sub>: 315.2, found: 316.1.

N-(1-Adamantyl)-2-(N-4'-trifluoromethoxyphenylamino)-acetamide (**53**). 276 mg (25%) of dark amber oil; <sup>1</sup>H NMR (CDCl<sub>3</sub>)  $\delta$  = 1.69 (6H, s), 2.0 (6H, s), 2.09 (3H, s), 3.74 (2H, s), 6.33 (1H, s), 6.75 (2H, s, J = 8 Hz), 7.71 (2H, s, J = 8 Hz); <sup>13</sup>C NMR (CDCl<sub>3</sub>)  $\delta$  = 29.37, 36.23, 41.48, 50.30, 52.07, 115.40, 122.50, 142.8, 167.73; ESI-MS [M+H]<sup>+</sup> calculated for  $C_{19}H_{23}F_{3}N_{2}O_{2}$ : 369.2, found: 369.3.

*N*-(1-Adamantyl)-2-(*N*-4'-trifluoromethylphenylamino)-acetamide (**54**). 296 mg (28%) of white powder; <sup>1</sup>H NMR (CDCl<sub>3</sub>)  $\delta$  = 1.69 (6H, s), 2.0 (6H, s), 2.1 (6H, s), 3.75 (2H, s), 6.07 (1H, s), 6.70 (2H, d, J = 8 Hz), 7.47 (2H, d, J = 8 Hz), <sup>13</sup>C NMR (CDCl<sub>3</sub>)  $\delta$  = 29.37, 36.23, 41.52, 48.89, 52.06, 113.02, 126.76, 149.31, 167.91; ESI-MS [M+H]<sup>+</sup> calculated for C<sub>19</sub>H<sub>23</sub>F<sub>3</sub>N<sub>2</sub>O: 353.2, found: 353.1.

*N*-(2-Adamantyl)-2-(*N*-4'-chlorophenylamino)acetamide (*55*). 673 mg (64%) of amber oil;  $^{1}$ H NMR (CDCl<sub>3</sub>)  $\delta$  = 1.63 (4H, s), 1.69–1.77 (3H, s), 1.79- 1.86 (8H, m), 3.74 (2H, s), 6.57 (2H, d, J = 8 Hz), 7.10 (2H, d, J = 8 Hz);  $^{13}$ C NMR (CDCl<sub>3</sub>)  $\delta$  = 27.07, 31.79, 37.05, 44.36, 50.88, 53.01, 55.36, 115.04, 116.69, 129.36, 144.41, 158.85, 169.69; ESI-MS [M+Na]<sup>+</sup> calculated for C<sub>18</sub>H<sub>23</sub>BClN<sub>2</sub>O: 343.1, found: 343.5.

*N*-(2-Adamantyl)-2-(*N*-4'-bromophenylamino)acetamide (**56**). 300 mg (31%) of amber oil;  $^{1}$ H NMR (CDCl<sub>3</sub>)  $\delta$  = 1.56 (4H, s), 1.71–1.76 (3H, m), 1.84–1.87 (8H, m), 3.79 (2H, s), 6.53 (2H, d, J = 12 Hz), 7.30 (2H, d, J = 8 Hz);  $^{13}$ C NMR (CDCl<sub>3</sub>)  $\delta$  = 27.05, 31.74, 31.93, 37.04, 37.40, 53.48, 132.49, 144.76, 173.50; ESI-MS [M +H]<sup>+</sup> calculated for C<sub>18</sub>H<sub>23</sub>BrN<sub>2</sub>O: 363.1, found: 363.3.

*N*-(2-Adamantyl)-2-(*N*-4'-methylphenylamino)acetamide (*57*). 232 mg (26%) of amber oil; <sup>1</sup>H NMR (CDCl<sub>3</sub>)  $\delta$  = 1.57 (4H, s), 1.71–1.75 (m, 3H), 1.85–1.89 (m, 8H), 2.27 (3H, s), 3.79 (2H, s), 6.58 (2H, d, J = 12 Hz), 7.03 (2H, d, J = 8 Hz); <sup>13</sup>C NMR (CDCl<sub>3</sub>)  $\delta$  = 20.43, 27.08, 30.95, 31.76, 37.06, 37.45, 49.83, 50.85, 52.84, 113.70, 119,67, 129.90, 144.74, 169.57; ESI-MS [M+H]<sup>+</sup> calculated for C<sub>19</sub>H<sub>26</sub>N<sub>2</sub>O: 299.2, found: 299.7.

N-(2-Adamantyl)-2-(N-4'-methoxyphenylamino)acetamide (**58**). 292 mg (31%) of amber oil;  ${}^{1}H$  NMR (CDCl<sub>3</sub>)  $\delta$  = 1.57 (4H, s), 1.71–1.75 (3H, m), 1.85–1.89 (8H, m), 3.78 (3H, s), 3.79 (2H, s), 6.64 (2H, d, J = 8 Hz), 6.80 (2H, d, J = 12 Hz);  ${}^{13}C$  NMR (CDCl<sub>3</sub>)  $\delta$  = 27.09, 31.78, 32.02, 37.04, 37.46, 50.23, 52.87, 55.72, 114.79, 114.90, 123.42, 140.99, 153.36, 169.47; ESI-MS [M+H]<sup>+</sup> calculated for  $C_{19}H_{26}N_2O$ : 315.2, found: 314.6.

N-(2-Adamantyl)-2-(N-4'-trifluoromethoxyphenylamino)-acetamide (**59**). 530 mg (43.6%) of amber oil;  ${}^{1}$ H NMR (CDCl<sub>3</sub>) δ = 1.56 (4H, s), 1.72–1.75 (3H, m), 1.84–1.88 (8H, m), 3.83 (2H, s), 6.66 (2H, d, J = 8 Hz), 7.0 (1H, s), 7.09 (2H, d, J = 8 Hz);  ${}^{13}$ C NMR (CDCl<sub>3</sub>) δ = 27.06, 31.74, 31.95, 37.04, 37.40, 49.83, 53.23, 63.85, 113.54, 115.39, 121.84, 122.56, 140.22, 144.20, 167.93;; ESI-MS [M +H]<sup>+</sup> calculated for C<sub>19</sub>H23F<sub>3</sub>N<sub>2</sub>O<sub>2</sub>: 369.2, found: 369.0.

N-(2-Adamantyl)-2-(N-4'-trifluoromethylphenylamino)-acetamide (**60**). 338 mg (32%) of amber oil;  ${}^{1}$ H NMR (CDCl<sub>3</sub>)  $\delta$  = 1.57 (4H, s), 1.72–1.77 (3H, m), 1.85–1.89 (8H, m), 3.88 (2H, s), 6.71 (2H, d, J = 8 Hz), 6.82 (1H, s), 7,47 (2H, d, J = 8 Hz);  ${}^{13}$ C NMR (CDCl<sub>3</sub>)  $\delta$  = 27.03, 31.78, 31.95, 37.02, 37.38, 48.52, 53.08, 112.89, 126.81, 136.53, 168.18; ESI-MS [M+H]+ calculated for  $C_{19}$ H23 $F_3$ N<sub>2</sub>O: 353.2, found: 353.4.

*N-(Cyclooctyl)-2-(N-4'-chlorophenylamino)acetamide* (*61*). 719 mg (68%) of pale yellow powder;  $^1$ H NMR (CDCl<sub>3</sub>)  $\delta$  = 1.48–1.57 (14H, m), 3.72 (2H, s), 4.03 (1H, m), 6.52 (2H, d, J = 8 Hz), 7.14 (2H, d, J = 12 Hz);  $^{13}$ C NMR (CDCl<sub>3</sub>)  $\delta$  = 23.53, 25.28, 27.13, 32.17, 49.04, 49.18, 114.38, 123.80, 129.27, 145.81, 168.45; ESI-MS [M +H]<sup>+</sup> calculated for C<sub>16</sub>H<sub>23</sub>ClN<sub>2</sub>O: 295.1, found: 295.3.

*N-(Cyclooctyl)-2-(N-4'-methylphenylamino)acetamide* (*62*). 527 mg (49%) of amber oil; <sup>1</sup>H NMR (CDCl<sub>3</sub>)  $\delta$  = 1.44–1.58 (14H, m), 2.24 (3H, s), 3.08 (2H, s), 3.71 (1H, s), 6.52 (2H, d, J = 8 Hz), 6.98 (2H, d, J = 8 Hz); <sup>13</sup>C NMR (CDCl<sub>3</sub>)  $\delta$  = 23.53, 25.27, 27.25, 32.01, 49.15, 50.58, 55.43, 113.37, 128.37, 129.85, 145.05, 169.60; ESI-MS [M+H]<sup>+</sup> calculated for C<sub>17</sub>H<sub>26</sub>N<sub>2</sub>O: 275.2, found: 275.5.

*N*-(*Cyclooctyl*)-2-(*N*-4'-methoxyphenylamino)acetamide (*63*). 592 mg (52%) of yellow powder;  $^{1}$ H NMR (CDCl<sub>3</sub>)  $\delta$  = 1.49–1.59 (14H, m), 3.72 (3H, s), 3.77 (2H, s), 4.04–4.06 (1H, m), 6.59 (2H, d, J = 12 Hz), 6.80 (2H, d, J = 8 Hz);  $^{13}$ C NMR (CDCl<sub>3</sub>)  $\delta$  = 23.54, 25.27, 27.17, 32.14, 49.04, 50.06, 55.72, 114.61, 114.91, 123.30, 141.20, 153.23, 169.17; ESI-MS [M+H]<sup>+</sup> calculated for C<sub>17</sub>H<sub>26</sub>N<sub>2</sub>O<sub>2</sub>: 291.2, found: 290.4.

*N-(Cyclooctyl)-2-(N-4'-trifluoromethoxyphenylamino)acetamide* (*64*). 595 mg (44%) of pale yellow powder;  $^{1}$ H NMR (CDCl<sub>3</sub>)  $\delta$  = 1.49–1.59 (14H, m), 3.76 (2H, s), 4.04–4.07 (1H, m), 6.51 (1H, d, J = 8 Hz), 6.58 (2H, d, J = 12 Hz), 7.07 (2H, d, J = 8 Hz);  $^{13}$ C NMR (CDCl<sub>3</sub>)  $\delta$  = 23.51, 25.28, 27.13, 32.14, 49.04, 49.21, 113.70, 122.53, 141.64, 146.02, 168.41; ESI-MS [M+H]<sup>+</sup> calculated for  $C_{17}H_{23}F_{3}N_{2}O_{2}$ : 345.2, found: 345.5.

*N*-(Cyclooctyl)-2-(*N*-4'-trifluoromethylphenylamino)acetamide (*65*). 590 mg (46%) of amber oil; <sup>1</sup>H NMR (CDCl<sub>3</sub>)  $\delta$  = 1.47–1.57 (14H, m), 3.78 (2H, s), 4.56–4.59 (1H, m), 6.28 (1H, s), 6.62 (2H, d, J = 8 Hz), 7.44 (2H, d, J = 8 Hz); <sup>13</sup>C NMR (CDCl<sub>3</sub>)  $\delta$  = 23.54, 25.30, 27.10, 32.17, 48.49, 49.43, 113.08, 126.82, 149.25, 167.70; ESI-MS [M+H]<sup>+</sup> calculated for C<sub>17</sub>H<sub>23</sub>F<sub>3</sub>N<sub>20</sub>: 329.2, found: 329.6.

*N*-(trans-Methylcyclohexyl)-2-(*N*-4'-chlorophenylamino)-acetamide (**66**). 396 mg (32%) of amber oil;  $^1$ H NMR (CDCl<sub>3</sub>)  $\delta$  = 0.89–0.91 (4H, m), 1.06–1.13 (4H, m), 1.69–1.75 (1H, m), 1.83–1.92 (3H, m), 3.81 (2H, s), 6.73 (2H, d, J = 8 Hz), 7.20 (2H, d, J = 8 Hz); ESI-MS [M+Na]<sup>+</sup> calculated for C<sub>16</sub>H<sub>24</sub>N<sub>2</sub>O: 303.1, found: 303.3.

*N*-(trans-Methylcyclohexyl)-2-(*N*-4'-methylphenylamino)-acetamide (**67**). 527 mg (47%) dark amber oil; <sup>1</sup>H NMR (CDCl<sub>3</sub>)  $\delta$  = 0.86–0.88 (2H, m), 1.02–1.09 (4H, m), 1.66–1.69 (2H, m), 1.80–1.84 (1H, m), 2.25 (3H, s), 3.72 (2H, s), 3.97–4.03 (1H, m), 6.51 (2H, d, J = 12 Hz), 7.01 (2H, d, J = 8 Hz); <sup>13</sup>C NMR (CDCl<sub>3</sub>)  $\delta$  = 20.46, 22.16, 31.84, 32.94, 33.77, 47.09, 48.29, 50.02, 60.89, 114.40, 129.96, 132.07, 169.05; ESI-MS [M+H]<sup>+</sup> calculated for C<sub>16</sub>H<sub>24</sub>N<sub>2</sub>O: 261.2, found: 261.4.

*N*-(1*R*,2*R*,3*R*,55)-(–)-IsopinocampheyI-2-(*N*-2'-chlorophenyI-amino)acetamide (**68**). 303 mg (29%) of amber oil; <sup>1</sup>H NMR (CDCl<sub>3</sub>)  $\delta$  = 0.77 (1H, d, J = 12 Hz); 1.07 (6H, s), 1.22 (3H, s), 1.67–1.69 (1H, m), 1.78–1.81 (1H, m), 1.91–1.95 (1H, m), 2.34–2.39 (1H, m), 2.56–2.62 (1H, m), 3.86 (2H, s), 4.30–4.37 (1H, m), 6.43 (1H, s), 6.58 (1H, d, J = 8 Hz), 6.77 (1H, t, J = 8 Hz), 7.17 (1H, t, J = 8 Hz), 7.31 (1H, d, J = 8 Hz); <sup>13</sup>C NMR (CDCl<sub>3</sub>)  $\delta$  = 20.67, 23,39, 28.01, 35.26, 36.91, 38.41, 41.49, 46.02, 47.66, 48.83, 112.03, 119.28, 119.81, 128.06, 129.32, 143.26, 169.0; ESI-MS [M+H]<sup>+</sup> calculated for C<sub>18</sub>H<sub>25</sub>ClN<sub>2</sub>O: 321.2, found: 321.0.

*N*-(1*R*,2*R*,3*R*,5*S*)-(–)-Isopinocampheyl-2-(*N*-3'-chlorophenyl-amino)acetamide (**69**). 260 mg (25%) of amber oil; <sup>1</sup>H NMR (CDCl<sub>3</sub>)  $\delta$  = 0.76 (1H, d, J = 8 Hz), 1.0 (3H, s), 1.04–1.06 (3H, m), 1.18 (3H, s), 1.44–1.49 (1H, m), 1.66–1.69 (1H, m), 1.74–1.77 (1H, m), 1.89–1.90 (1H, m), 2.31–2.36 (1H, m), 2.50–2.56 (1H, m), 3.74–3.78 (1H, m), 4.26–4.34 (1H, m), 4.94–4.96 (1H, m), 6.46 (1H, d, J = 8 Hz), 6.59 (1H, s), 6.71 (1H, d, J = 8 Hz), 7.06 (1H, t, J = 8 Hz); <sup>13</sup>C NMR (CDCl<sub>3</sub>)  $\delta$  = 20.7, 23.33, 27.97, 35,18, 36.81, 38.36, 41.45, 45.88, 47.61, 48.48, 11.36, 113.31, 118.55, 130.35, 135.02, 148.64, 169.37; ESI-MS [M+H]<sup>+</sup> calculated for C<sub>18</sub>H<sub>25</sub>ClN<sub>2</sub>O: 321.2, found: 323.3.

 s), 1.45–1.50 (1H, m), 1.69–1.70 (1H, m), 1.93–1.96 (1H, m), 2.35–2.40 (1H, m), 2.57–2.63 (1H, m), 3.79 (2H, s), 4.31–4.38 (1H, m), 4.46 (1H, s), 6.39 (1H, s), 6.54 (1H, d, J = 8 Hz), 6.79 (1H, d, J = 4 Hz), 6.92 (1H, d, J = 8 Hz), 7.07 (1H, t, J = 8 Hz); <sup>13</sup>C NMR (CDCl<sub>3</sub>)  $\delta = 20.67$ , 23.38, 28.0, 35.30, 36.96, 38.40, 41.49, 46.16, 47.64, 48.64, 111.87, 116.15, 121.89, 123.33, 130.70, 148.5, 168.91; ESI-MS [M+H]<sup>+</sup> calculated for C<sub>18</sub>H<sub>2</sub>, BrN<sub>2</sub>O: 365.1, found: 365.2.

*N*-(1-Adamantyl)-2-(*N*-2'-chlorophenylamino)acetamide (*71*). 357 mg (34%) of amber oil;  ${}^{1}H$  NMR (CDCl<sub>3</sub>)  $\delta$  = 1.70 (6H, s), 2.00 (6H, s), 2.09 (3H, s), 3.76 (2H, s), 6.61 (1H, d, J = 8 Hz), 6.77 (1H, t, J = 8 Hz), 7.19 (1H, t, J = 8 Hz), 7.31 (1H, d, J = 8 Hz);  ${}^{13}C$  NMR (CDCl<sub>3</sub>)  $\delta$  = 29.38, 36.26, 41.51, 49.13, 51.84, 111.46, 113.26, 118.87, 130.39, 135.13, 148.37, 168.45; ESI-MS [M+H]<sup>+</sup> calculated for  $C_{18}H_{23}ClN_2O$ : 319.2, found: 319.3.

*N*-(1-Adamantyl)-2-(*N*-3'-chlorophenylamino)acetamide (**72**). 305 mg (29%) of amber oil; <sup>1</sup>H NMR (CDCl<sub>3</sub>)  $\delta$  = 1.68 (6H, s), 1.99 (6H, s), 2.06 (3H, s), 3.66 (2H, s), 6.21 (1H, s), 6.48 (1H, d, J = 8 Hz), 6.61 (1H, s), 6.76 (1H, d, J = 8 Hz), 7.12 (1H, t, J = 8 Hz); <sup>13</sup>C NMR (CDCl<sub>3</sub>)  $\delta$  = 29.37, 36.25, 41.49, 49.11, 51.82, 111.42, 113.42, 118.76, 130.39, 135.09, 148.46, 168.60; ESI-MS [M+H]<sup>+</sup> calculated for C<sub>18</sub>H<sub>23</sub>ClN<sub>2</sub>O: 319.2, found: 319.1.

*N*-(1-Adamantyl)-2-(*N*-2'-bromophenylamino)acetamide (**73**). 372 mg (31%) of amber oil;  $^{1}$ H NMR (CDCl<sub>3</sub>)  $\delta$  = 1.68 (6H, s), 2.0 (6H, s), 2.08 (3H, s), 3.74 (2H, s), 6.20 (1H, s), 6.57 (1H, d, J = 8 Hz), 6.71 (1H, t, J = 8 Hz), 7.23 (1H, t, J = 8 Hz), 7.47 (1H, d, J = 8 Hz); ESI-MS [M+H]<sup>+</sup> calculated for C<sub>18</sub>H<sub>23</sub>BrN<sub>2</sub>O: 364.3, found: 363.1.

*N*-(1-Adamantyl)-2-(*N*-3'-bromophenylamino)acetamide (**74**). 383 mg (32%) of amber oil; <sup>1</sup>H NMR (CDCl<sub>3</sub>)  $\delta$  = 1.68 (6H, s), 1.99 (6H, s), 2.06 (3H, s), 3.65 (2H, s), 6.20 (1H, s), 6.52 (1H, d, J = 8 Hz), 6.77 (1H, t, J = 4 Hz), 6.90 (1H, d, J = 8 Hz), 7.06 (1H, t, J = 8 Hz); <sup>13</sup>C NMR (CDCl<sub>3</sub>)  $\delta$  = 29.37, 36.25, 41.49, 49.07, 51.84, 111.84, 116.15, 121.66, 123.26, 130.67, 148.59, 168.56; ESI-MS [M +H]<sup>+</sup> calculated for C<sub>18</sub>H<sub>23</sub>BrN<sub>2</sub>O: 364.3, found: 364.9.

*N*-(1-Adamantyl)-2-(N-2'-trifluoromethoxyphenylamino)-acetamide (**75**). 352 mg (29%) of amber oil;  ${}^{1}$ H NMR (CDCl<sub>3</sub>)  $\delta$  = 1.68 (6H, s), 1.97 (6H, s), 2.07 (3H, s), 3.74 (2H, s), 6.24 (1H, s), 6.65 (1H, d, J = 8 Hz), 6.81 (1H, t, J = 8 Hz), 7.18–7.22 (2H, m);  ${}^{13}$ C NMR (CDCl<sub>3</sub>)  $\delta$  = 29.36, 36.23, 41.39, 48.67, 51.66, 112.53, 118.42, 128.01, 136.42, 139.61, 168.45; ESI-MS [M+H]<sup>+</sup> calculated for C<sub>19</sub>H<sub>23</sub>F<sub>3</sub>N<sub>2</sub>O<sub>2</sub>: 369.2, found: 369.2.

*N*-(1-Adamantyl-(3-trifluoromethoxyphenylamino)acetamide (**76**). 29 mg (37.6%) of amber oil; <sup>1</sup>H NMR (CDCl<sub>3</sub>)  $\delta$  = 1.68 (6H, s), 1.99 (6H, s), 2.06 (3H, s), 3.68 (2H, s), 4.57 (1H, s), 6.45 (1H, s), 6.53 (1H, d, J = 8 Hz), 6.64 (1H, d, J = 8 Hz), 7.20 (1H, t, J = 8 Hz); <sup>13</sup>C NMR (CDCl<sub>3</sub>)  $\delta$  = 29.37, 36.23, 41.48, 49.10, 51.86, 105.69, 110.74, 111.57, 130.39, 148.75, 150.37, 168.44; ESI-MS [M+H]<sup>+</sup> calculated for C<sub>19</sub>H<sub>23</sub>F<sub>3</sub>N<sub>2</sub>O<sub>2</sub>: 369.2, found: 369.0.

**cLogP Calculation.** cLogP values were generated using ChemDraw Prime v15.1.

Kinetic Solubility Assay.<sup>36</sup> A stock solution of each active compound in DMSO (10 mg/mL) was prepared, diluted into physiological buffer (pH = 7.4) at a concentration of 100  $\mu$ g/mL, and left for 6 h at room temperature. This experiment was run in triplicate. After 6 h, the sample was centrifuged, and the supernatant was diluted with a methanol—water solution containing internal standard (IS). The calibration curve was established with seven-point standards, prepared by a serial dilution in the range the unknown sample signal would likely fall and exactly simulating the sample preparation. The standards and samples were quantified using LC-MS/MS, and unknown concentrations were back-calculated from the calibration curve

PAMPA Permeability Assay.<sup>36</sup> Parallel artificial membrane permeability assay (PAMPA), with an artificial membrane that simulates a biological membrane, was used. A 96-well membrane-filter-based microtiter plate system with donor and acceptor compartments separated by the membrane was employed. The compounds were dissolved in 5% DMSO in phosphate-buffered saline (PBS) solution with Lucifer yellow, a dye used to assess membrane integrity. The solution was placed in the donor well, and PBS was

added to the acceptor well. The membrane was generated by dissolving lecithin in an inert organic solvent and placed onto a hydrophobic PVDF filter. The plates were then allowed to incubate for 16 h. This assay was run in triplicate. For each compound, a concentration versus area ratio calibration curve with seven points was plotted, and the concentrations of the compounds in the donor and acceptor compartments were quantified using the calibration curve on an HPLC. The apparent permeability ( $P_e$ , cm/s) was calculated using the following formula.

$$P_{\rm e} = \left[ \frac{V_{\rm D} \times V_{\rm A}}{(V_{\rm D} + V_{\rm A}) \times \text{Area} \times \text{Time}} \right] \times \left\{ -\ln \left[ 1 - \frac{C_{\rm A}(t)}{C_{\rm eq}} \right] \right\} \tag{1}$$

 $V_{\rm D}$  = donor compartment volume (0.15 mL)

 $V_{\rm A}$  = acceptor compartment volume (0.3 mL)

Area = area of the membrane  $(0.3 \text{ cm}^2)$ 

Time = time of incubation (57,600 s)

 $C_{\rm A}(t)=$  the concentration of solution in the acceptor chamber after 16 h

 $C_{\text{eq}}$  = the equilibrium concentration

Human Plasma Protein Binding. The rapid equilibrium dialysis (RED) method was used. The compounds were spiked with human plasma at 10  $\mu$ g/mL concentrations and placed in plasma chambers of the RED device. PBS was placed in the buffer chambers, and the RED device was sealed and allowed to shake in an orbital shaker for 4 h at 37 °C to achieve equilibrium. Equal volumes of plasma were added to the aliquots of the buffer chambers and vice versa to create identical matrices. The compounds were then precipitated using methanol (4 times the aqueous phase) and centrifuged, then the compound concentration in the supernatant was quantified using LC/MS/MS. This assay was performed in triplicate. The % free and bound drug concentrations were calculated using eqs 2 and 3, respectively.

$$%Free = \frac{[buffer\ chamber\ compound\ concentration]}{[plasma\ chamber\ compound\ concentration]} \times 100$$

(2)

$$\%Bound = 100 - \%Free \tag{3}$$

**Metabolic Stability Assay.** The metabolic stability of the prodrug was assessed in a mouse liver S9 fraction. Briefly, 5  $\mu$ g/mL of prodrug was incubated with 1 mg/mL mouse liver S9 fraction supplemented with 1 mg/mL nicotinamide adenine dinucleotide phosphate (NADPH) in Dulbecco's phosphate-buffered saline at 37 °C. At designated time points (i.e., 0, 0.5, 1, 2, and 5 h), 100  $\mu$ L samples were collected and quenched immediately with 300  $\mu$ L acetonitrile containing 1  $\mu$ g/mL internal standard. Samples were vortexed for 30 s and centrifuged at 15,000 rpm for 10 min. Supernatant was assessed by LC/MS. This assay was performed in triplicate.

Cytotoxicity. WI-26 VA4 cell lines were cultured and grown per the ATCC protocol (ATCC, 2019). The MTT assay was performed following the Vybrant MTT assay protocol (Vybrant cell proliferation protocol, 2002). Briefly, the trypsinized cells were seeded in each well of a 96-well plate in a 37 °C incubator with 5% CO2. Active compounds were prepared by serial dilution from 20  $\mu$ g/mL to  $0.00002 \mu g/mL$  with 10-fold dilutions using MEM/FBS with 0.2% DMSO. After 24 h, when the cell confluency was 10-15%, the media was replaced with 100  $\mu$ L of freshly prepared dilutions of acetamides, and this was performed in triplicate. The cells were allowed to grow for 72 h. After 72 h, the media was replaced by MEM/FBS, and 10  $\mu$ L of 5 mg/mL MTT in sterile PBS was added to each well. The plates were incubated at 37 °C for 4 h. After 4 h, the treatment, media, and MTT reagent were replaced by sodium dodecylsulfate (SDS) in 0.01 M HCl solution to aid in dissolution of formazan crystals. The dissolved formazan was incubated at 37  $^{\circ}\text{C}$  for 30 min and shaken in an orbital shaker for another 30 min to ensure the dissolution of formazan crystals. The absorbance of dissolved formazan was measured using a plate reader at 570 nm. One set of wells were

(4)

untreated controlled wells, where cells in MEM/10% FBS with 0.2% DMSO without the compounds were placed. The percentage cell viability was calculated using the following equation.

$$% Cell Viability = \frac{absorbance of sample}{absorbance of untreated control} \times 100\%$$

**MIC Testing.** The MIC values were determined by the microbroth dilution method. Briefly, M.tb H37Rv mc2 6206 was grown in Middlebrook 7H9 media, and NTM pathogens were grown in Mueller Hinton II (BD) media by incubating at 37 °C until the optical density (OD) reached 0.08–0.1. The compound was dissolved in DMSO at a concentration of 10 mg/mL and stored at -80 °C until required. 100  $\mu$ L of the compound, 2-fold serially diluted in Middlebrook 7H9 starting from 64  $\mu$ g/mL, was added to the 96-well microtiter plates. 100  $\mu$ L of the culture of these mycobacteria was added to the drug plates and incubated at 37 °C for 5 days (M.abs) or 7 days (M.tb). The plates were then visually inspected for bacterial growth to determine the MIC value. This assay was performed in duplicate and repeated.

**Mechanism of Action Studies.** MIC determinations against *M.smg* expressing mutated variants of MmpL3tb and MmpL3abs, metabolic labeling, fluorescent probe displacement assays, and SPR were conducted as described in our earlier study.<sup>31</sup>

**Molecular Docking.** Ligand structures were sketched using ChemDraw and Chem3D. Each structure was drawn in ChemDraw first, after which the ligand structures were optimized in Chem3D using MM2 energy minimization up to 0.01 gradient, and then exported in the mol2 format. The crystal structure of MmpL3 was taken from the Protein Data Bank (PDB ID: 6AJG). <sup>12</sup>

Following the guidance in Forli et al.,<sup>38</sup> we used AutoDock Vina<sup>39,40</sup> for further preparation and flexible docking. The flexible residues we chose were Asp256, Tyr257, Ser293, Ile297, Leu642, Asp645, and Tyr646. After adding hydrogens to the MmpL3 crystal structure, two receptor files were generated based on the residue choices, each of which contained only the rigid part or only the flexible part. The center of the grid box was determined by the position of the SQ109 ligand in the crystal structure, while the size of the box is (30 Å)<sup>3</sup>. The Vina forcefield with exhaustiveness parameter 32 was used to apply flexible docking to 10 ligands. The docking results were analyzed using the online tool PLIP<sup>41</sup> to identify protein—ligand interactions, and PyMOL as well as VMD<sup>42</sup> were used for visualization.

#### ASSOCIATED CONTENT

#### Supporting Information

The Supporting Information is available free of charge at https://pubs.acs.org/doi/10.1021/acs.jmedchem.2c00352.

Results and discussion for pyrrole-, imidazole-, and mandelic acid-based compounds (PDF)

Compound SMILES and biological data (CSV)

#### AUTHOR INFORMATION

#### **Corresponding Author**

E. Jeffrey North — Department of Pharmacy Sciences, Creighton University, Omaha, Nebraska 68178, United States; orcid.org/0000-0001-7644-030X; Phone: (402) 280-2871; Email: jeffreynorth@creighton.edu

#### **Authors**

Pankaj Bhattarai – Department of Pharmacy Sciences, Creighton University, Omaha, Nebraska 68178, United States

**Pooja Hegde** – Department of Pharmacy Sciences, Creighton University, Omaha, Nebraska 68178, United States

Wei Li – Mycobacteria Research Laboratories, Department of Microbiology, Immunology and Pathology, Colorado State University, Fort Collins, Colorado 80523, United States

Pavan Kumar Prathipati – Department of Pharmacy Sciences, Creighton University, Omaha, Nebraska 68178, United States

Casey M. Stevens – Department of Chemistry and Biochemistry, University of Oklahoma, Norman, Oklahoma 73019, United States

Lixinhao Yang — School of Chemistry and Biochemistry, Georgia Institute of Technology, Atlanta, Georgia 30332, United States

Hinman Zhou – Department of Pharmacy Sciences, Creighton University, Omaha, Nebraska 68178, United States

Amit Pandya – Department of Pharmacy Sciences, Creighton University, Omaha, Nebraska 68178, United States

Katie Cunningham – Department of Pharmacy Sciences, Creighton University, Omaha, Nebraska 68178, United States

Jenny Grissom – Department of Pharmacy Sciences, Creighton University, Omaha, Nebraska 68178, United States

Mariaelena Roman Sotelo – Department of Pharmacy Sciences, Creighton University, Omaha, Nebraska 68178, United States

Melanie Sowards – Department of Pharmacy Sciences, Creighton University, Omaha, Nebraska 68178, United States

Lilian Calisto – Department of Oral Biology, Creighton University, Omaha, Nebraska 68178, United States

Christopher J. Destache – Department of Pharmacy Practice, Creighton University, Omaha, Nebraska 68178, United States

Sonia Rocha-Sanchez — Department of Oral Biology, Creighton University, Omaha, Nebraska 68178, United States

James C. Gumbart — School of Physics and School of Chemistry and Biochemistry, Georgia Institute of Technology, Atlanta, Georgia 30332, United States; orcid.org/0000-0002-1510-7842

Helen I. Zgurskaya — Department of Chemistry and Biochemistry, University of Oklahoma, Norman, Oklahoma 73019, United States; orcid.org/0000-0001-8929-4727

Mary Jackson — Mycobacteria Research Laboratories, Department of Microbiology, Immunology and Pathology, Colorado State University, Fort Collins, Colorado 80523, United States; orcid.org/0000-0002-9212-0258

Complete contact information is available at: https://pubs.acs.org/10.1021/acs.jmedchem.2c00352

#### **Author Contributions**

\*P.B. and P.H. contributed equally to this study.

#### Notes

The authors declare no competing financial interest.

#### ACKNOWLEDGMENTS

Research reported in this publication was supported by the National Institutes of Health/National Institute of Allergy and Infectious Diseases research grant AI116525, the Translational Hearing Center Creighton University Center of Biomedical Research Excellence (COBRE) of the National Institutes of Health under grant number 1P20GM139762-01, the Health

Science Strategic Investment Fund Faculty Development Grant, the Cystic Fibrosis Foundation (NORTH18I0), and the Jack and Lois Wareham Research Award. The authors would also like to thank the Department of Chemistry at Creighton University for the use of their NMR and Dr. William Jacobs (Albert Einstein College of Medicine, NY, USA) for the provision of *M. tuberculosis* H37Rv mc<sup>2</sup>6206.

#### ABREVIATIONS USED

BCS, Biopharmaceutical Classification System; COPD, chronic obstructive pulmonary disease; EDC·HCl, 1-ethyl-3-(3-(dimethylamino)propyl)carbodiimide hydrochloride; HOBt, hydroxybenzotriazole; HPPB, human plasma protein binding; IC, indole-2-carboxamide; M., Mycobacterium; M.tb, Mycobacterium tuberculosis; MAC, Mycobacterium avium complex; MABSC, Mycobacterium abscessus complex; MIC, minimum inhibitory concentration; MDR-TB, multi-drug-resistant tuberculosis; MFI, mean fluorescence intensity; MmpL3, mycobacteria membrane protein large 3; NTM, non-tuberculous mycobacteria; PC, pyrrole-2-carboxamide; RED, rapid equilibrium dialysis; RND, resistance nodulation cell division; SAR, structure-activity relationship; SPR, surface plasmon resonance; TMM, trehalose monomycolate; USP, United States Pharmacopeia; XDR-TB, extensively drug-resistant tuberculosis

#### REFERENCES

- (1) Ahmad, S. Pathogenesis, immunology, and diagnosis of latent Mycobacterium tuberculosis infection. *Clin. Dev. Immunol.* **2011**, 2011, 814943.
- (2) Global Tuberculosis Report 2019. World Health Organization, May 5, 2020. https://www.who.int/publications/m/item/global-tuberculosis-report-2019
- (3) Faria, S.; Joao, I.; Jordao, L. General overview on nontuberculous mycobacteria, biofilms, and human infection. *J. Pathogens* **2015**, 2015, 800014
- (4) Van der Werf, M. J.; Ködmön, C.; Katalinić-Janković, V.; Kummik, T.; Soini, H.; Richter, E.; Papaventsis, D.; Tortoli, E.; Perrin, M.; van Soolingen, D.; et al. Inventory study of nontuberculous mycobacteria in the European Union. *BMC Infect. Dis.* **2014**, *14* (1), 62.
- (5) Lin, C.; Russell, C.; Soll, B.; Chow, D.; Bamrah, S.; Brostrom, R.; Kim, W.; Scott, J.; Bankowski, M. J. Increasing Prevalence of Nontuberculous Mycobacteria in Respiratory Specimens from US-Affiliated Pacific Island Jurisdictions. *Emerg. Infect. Dis.* **2018**, 24 (3), 485–491.
- (6) Santin, M.; Barrabeig, I.; Malchair, P.; Gonzalez-Luquero, L.; Benitez, M. A.; Sabria, J.; Palau-Benavent, M.; Cañete, C.; Lloret-Queraltó, J. A.; Grijota-Camino, M. D.; et al. Pulmonary Infections with Nontuberculous Mycobacteria, Catalonia, Spain, 1994–2014. *Emerg. Infect. Dis.* **2018**, 24 (6), 1091–1094.
- (7) Franz, N. D.; Belardinelli, J. M.; Kaminski, M. A.; Dunn, L. C.; Calado Nogueira de Moura, V.; Blaha, M. A.; Truong, D. D.; Li, W.; Jackson, M.; North, E. J. Design, synthesis and evaluation of indole-2-carboxamides with pan anti-mycobacterial activity. *Bioorg. Med. Chem.* 2017, 25 (14), 3746–3755.
- (8) Torfs, E.; Piller, T.; Cos, P.; Cappoen, D. Opportunities for Overcoming Mycobacterium tuberculosis Drug Resistance: Emerging Mycobacterial Targets and Host-Directed Therapy. *Int. J. Mol. Sci.* **2019**, 20 (12), 2868.
- (9) Belardinelli, J. M.; Yazidi, A.; Yang, L.; Fabre, L.; Li, W.; Jacques, B.; Angala, S. K.; Rouiller, I.; Zgurskaya, H. I.; Sygusch, J.; Jackson, M. Structure-Function Profile of MmpL3, the Essential Mycolic Acid Transporter from Mycobacterium tuberculosis. *ACS Infect. Dis.* **2016**, 2 (10), 702–713.

- (10) Li, W.; Upadhyay, A.; Fontes, F. L.; North, E. J.; Wang, Y.; Crans, D. C.; Grzegorzewicz, A. E.; Jones, V.; Franzblau, S. G.; Lee, R. E.; et al. Novel insights into the mechanism of inhibition of MmpL3, a target of multiple pharmacophores in Mycobacterium tuberculosis. *Antimicrob. Agents Chemother.* **2014**, 58, 6413–6423.
- (11) Grzegorzewicz, A. E.; Pham, H.; Gundi, V. A.; Scherman, M. S.; North, E. J.; Hess, T.; Jones, V.; Gruppo, V.; Born, S. E.; Korduláková, J.; et al. Inhibition of mycolic acid transport across the Mycobacterium tuberculosis plasma membrane. *Nat. Chem. Biol.* **2012**, *8* (4), 334–341.
- (12) Zhang, B.; Li, J.; Yang, X.; Wu, L.; Zhang, J.; Yang, Y.; Zhao, Y.; Zhang, L.; Yang, X.; Yang, X.; Cheng, X.; Liu, Z.; Jiang, B.; Jiang, H.; Guddat, L. W.; Yang, H.; Rao, Z. Crystal Structures of Membrane Transporter MmpL3, an Anti-TB Drug Target. *Cell* **2019**, *176* (3), 636–648.
- (13) Brown, J. R.; North, E. J.; Hurdle, J. G.; Morisseau, C.; Scarborough, J. S.; Sun, D.; Kordulakova, J.; Scherman, M. S.; Jones, V.; Grzegorzewicz, A.; Crew, R. M.; Jackson, M.; McNeil, M. R.; Lee, R. E. The structure-activity relationship of urea derivatives as antituberculosis agents. *Bioorg. Med. Chem.* **2011**, *19* (18), 5585–5595.
- (14) Lun, S.; Guo, H.; Onajole, O. K.; Pieroni, M.; Gunosewoyo, H.; Chen, G.; Tipparaju, S. K.; Ammerman, N. C.; Kozikowski, A. P.; Bishai, W. R. Indoleamides are active against drug-resistant Mycobacterium tuberculosis. *Nat. Commun.* **2013**, *4*, 2907.
- (15) North, E. J.; Scherman, M. S.; Bruhn, D. F.; Scarborough, J. S.; Maddox, M. M.; Jones, V.; Grzegorzewicz, A.; Yang, L.; Hess, T.; Morisseau, C.; Jackson, M.; McNeil, M. R.; Lee, R. E. Design, synthesis and anti-tuberculosis activity of 1-adamantyl-3-heteroaryl ureas with improved in vitro pharmacokinetic properties. *Bioorg. Med. Chem.* **2013**, 21 (9), 2587–2599.
- (16) Pandya, A. N.; Prathipati, P. K.; Hegde, P.; Li, W.; Graham, K. F.; Mandal, S.; Drescher, K. M.; Destache, C. J.; Ordway, D.; Jackson, M.; North, E. J. Indole-2-carboxamides are Active Against an Acute Mycobacterium abscessus Infected Mouse Model. *Antimicrob. Agents Chemother.* **2019**, *63*, No. e02245-18.
- (17) Stec, J.; Onajole, O. K.; Lun, S.; Guo, H.; Merenbloom, B.; Vistoli, G.; Bishai, W. R.; Kozikowski, A. P. Indole-2-carboxamide-Based MmpL3 Inhibitors Show Exceptional Antitubercular Activity in an Animal Model of Tuberculosis Infection. *J. Med. Chem.* **2016**, *59* (13), 6232–6247.
- (18) Matta, C. F.; Arabi, A. A.; Weaver, D. F. The bioisosteric similarity of the tetrazole and carboxylate anions: Clues from the topologies of the electrostatic potential and of the electron density. *Eur. J. Med. Chem.* **2010**, *45* (5), 1868–1872.
- (19) Kondreddi, R. R.; Jiricek, J.; Rao, S. P.; Lakshminarayana, S. B.; Camacho, L. R.; Rao, R.; Herve, M.; Bifani, P.; Ma, N. L.; Kuhen, K.; Goh, A.; Chatterjee, A. K.; Dick, T.; Diagana, T. T.; Manjunatha, U. H.; Smith, P. W. Design, synthesis, and biological evaluation of indole-2-carboxamides: a promising class of antituberculosis agents. *J. Med. Chem.* **2013**, *56* (21), 8849–8859.
- (20) Kozikowski, A. P.; Onajole, O. K.; Stec, J.; Dupont, C.; Viljoen, A.; Richard, M.; Chaira, T.; Lun, S.; Bishai, W.; Raj, V. S.; Ordway, D.; Kremer, L. Targeting Mycolic Acid Transport by Indole-2-carboxamides for the Treatment of Mycobacterium abscessus Infections. *J. Med. Chem.* **2017**, *60* (13), 5876–5888.
- (21) Onajole, O. K.; Pieroni, M.; Tipparaju, S. K.; Lun, S.; Stec, J.; Chen, G.; Gunosewoyo, H.; Guo, H.; Ammerman, N. C.; Bishai, W. R.; Kozikowski, A. P. Preliminary structure-activity relationships and biological evaluation of novel antitubercular indolecarboxamide derivatives against drug-susceptible and drug-resistant *Mycobacterium tuberculosis* strains. *J. Med. Chem.* **2013**, *56*, 4093–4103.
- (22) Shetty, A.; Xu, Z.; Lakshmanan, U.; Hill, J.; Choong, M. L.; Chng, S.-S.; Yamada, Y.; Poulsen, A.; Dick, T.; Gengenbacher, M. Novel Acetamide Indirectly Targets Mycobacterial Transporter MmpL3 by Proton Motive Force Disruption. *Front. Microbiol.* **2018**, 9, 2960.
- (23) Lovering, F.; Bikker, J.; Humblet, C. Escape from flatland: increasing saturation as an approach to improving clinical success. *J. Med. Chem.* **2009**, *52* (21), *6752*–*6756*.

- (24) Lovering, F. Escape from Flatland 2: complexity and promiscuity. *MedChemComm* **2013**, 4 (3), 515–519.
- (25) Ishikawa, M.; Hashimoto, Y. Improvement in aqueous solubility in small molecule drug discovery programs by disruption of molecular planarity and symmetry. *J. Med. Chem.* **2011**, *54* (6), 1539–1554.
- (26) Ranitidine. DrugBank Online, drug created Jun 13, 2005. https://go.drugbank.com/drugs/DB00863(accessed Mar 29, 2021).
- (27) Alvarez-Figueroa, M. J.; Pessoa-Mahana, C. D.; Palavecino-González, M. E.; Mella-Raipán, J.; Espinosa-Bustos, C.; Lagos-Muñoz, M. E. Evaluation of the membrane permeability (PAMPA and skin) of benzimidazoles with potential cannabinoid activity and their relation with the Biopharmaceutics Classification System (BCS). AAPS PharmSciTech 2011, 12 (2), 573–578.
- (28) Benet, L. Z. The role of BCS (biopharmaceutics classification system) and BDDCS (biopharmaceutics drug disposition classification system) in drug development. *J. Pharm. Sci.* **2013**, *102* (1), 34–42.
- (29) Varma, M. V.; Gardner, I.; Steyn, S. J.; Nkansah, P.; Rotter, C. J.; Whitney-Pickett, C.; Zhang, H.; Di, L.; Cram, M.; Fenner, K. S.; El-Kattan, A. F. pH-Dependent solubility and permeability criteria for provisional biopharmaceutics classification (BCS and BDDCS) in early drug discovery. *Mol. Pharmaceutics* 2012, 9 (5), 1199–1212.
- (30) Yu, H.; Wang, Q.; Sun, Y.; Shen, M.; Li, H.; Duan, Y. A new PAMPA model proposed on the basis of a synthetic phospholipid membrane. *PloS one* **2015**, *10* (2), No. e0116502.
- (31) Li, W.; Stevens, C. M.; Pandya, A. N.; Darzynkiewicz, Z.; Bhattarai, P.; Tong, W.; Gonzalez-Juarrero, M.; North, E. J.; Zgurskaya, H. I.; Jackson, M. Direct Inhibition of MmpL3 by Novel Antitubercular Compounds. *ACS Infect. Dis.* **2019**, *5*, 1001–1012.
- (32) Stevens, C. M.; Babii, S. O.; Pandya, A. N.; Li, W.; Li, Y.; Mehla, J.; Scott, R.; Hegde, P.; Prathipati, P. K.; Acharya, A.; Liu, J.; Gumbart, J. C.; North, J.; Jackson, M.; Zgurskaya, H. I. Proton transfer activity of the reconstituted Mycobacterium tuberculosis MmpL3 is modulated by substrate mimics and inhibitors. *Proc. Natl. Acad. Sci. U. S. A.* 2022, 119 (30), No. e2113963119.
- (33) Yang, X.; Hu, T.; Yang, X.; Xu, W.; Yang, H.; Guddat, L. W.; Zhang, B.; Rao, Z. Structural Basis for the Inhibition of Mycobacterial MmpL3 by NITD-349 and SPIRO. *J. Mol. Biol.* **2020**, 432 (16), 4426–4434.
- (34) Deshpande, D.; Srivastava, S.; Meek, C.; Leff, R.; Gumbo, T. Ethambutol Optimal Clinical Dose and Susceptibility Breakpoint Identification by Use of a Novel Pharmacokinetic-Pharmacodynamic Model of Disseminated Intracellular Mycobacterium avium. *Antimicrob. Agents Chemother.* **2010**, *54* (5), 1728–1733.
- (35) Suo, J.; Chang, C. E.; Lin, T. P.; Heifets, L. B. Minimal inhibitory concentrations of isoniazid, rifampin, ethambutol, and streptomycin against Mycobacterium tuberculosis strains isolated before treatment of patients in Taiwan. *Am. Rev. Respiratory Dis.* 1988, 138 (4), 999–1001.
- (36) North, E. J.; Scherman, M. S.; Bruhn, D. F.; Scarborough, J. S.; Maddox, M. M.; Jones, V.; Grzegorzewicz, A.; Yang, L.; Hess, T.; Morisseau, C.; Jackson, M.; McNeil, M. R.; Lee, R. E. Design, synthesis and anti-tuberculosis activity of 1-adamantyl-3-heteroaryl ureas with improved in vitro pharmacokinetic properties. *Biorg. Med. Chem.* **2013**, *21* (9), 2587–2599.
- (37) Faller, B. Artificial membrane assays to assess permeability. *Curr. Drug Metab.* **2008**, *9* (9), 886–892.
- (38) Forli, S.; Huey, R.; Pique, M. E.; Sanner, M. F.; Goodsell, D. S.; Olson, A. J. Computational protein-ligand docking and virtual drug screening with the AutoDock suite. *Nat. Protoc.* **2016**, *11* (5), 905–19.
- (39) Eberhardt, J.; Santos-Martins, D.; Tillack, A. F.; Forli, S. AutoDock Vina 1.2.0: New Docking Methods, Expanded Force Field, and Python Bindings. *J. Chem. Inf. Model.* **2021**, *61* (8), 3891–3898. (40) Trott, O.; Olson, A. J. AutoDock Vina: improving the speed and accuracy of docking with a new scoring function, efficient optimization, and multithreading. *J. Comput. Chem.* **2009**, *31* (2), 455–461.

- (41) Adasme, M. F.; Linnemann, K. L.; Bolz, S. N.; Kaiser, F.; Salentin, S.; Haupt, V. J.; Schroeder, M. PLIP 2021: expanding the scope of the protein-ligand interaction profiler to DNA and RNA. *Nucleic Acids Res.* **2021**, *49* (W1), W530–W534.
- (42) Humphrey, W.; Dalke, A.; Schulten, K. VMD: visual molecular dynamics. J. Mol. Graph. 1996, 14 (1), 33–38.

### **□** Recommended by ACS

Investigation into the Mechanism of Action of the Tuberculosis Drug Candidate SQ109 and Its Metabolites and Analogues in Mycobacteria

Satish R. Malwal, Eric Oldfield, et al.

MAY 26, 2023

JOURNAL OF MEDICINAL CHEMISTRY

DEAD E

#### Discovery of 5-Phenylpyrazolopyrimidinone Analogs as Potent Antitrypanosomal Agents with In Vivo Efficacy

Yang Zheng, Rob Leurs, et al.

JULY 20, 2023

JOURNAL OF MEDICINAL CHEMISTRY

READ 🗹

## Basic Nitrogen (BaN) Is a Key Property of Antimalarial Chemical Space

Harsha Valluri, Sandeep Sundriyal, et al.

JUNE 25, 2023

JOURNAL OF MEDICINAL CHEMISTRY

READ [7

#### Structure-Guided Design and Synthesis of a Pyridazinone Series of *Trypanosoma cruzi* Proteasome Inhibitors

Michael G. Thomas, Manu De Rycker, et al.

JULY 28, 2023

JOURNAL OF MEDICINAL CHEMISTRY

READ 🗹

Get More Suggestions >